NV5 GEOSPATIAL
powered by QUANTUM SPATIAL

November 24, 2021,
Revision 1: February 14, 2022

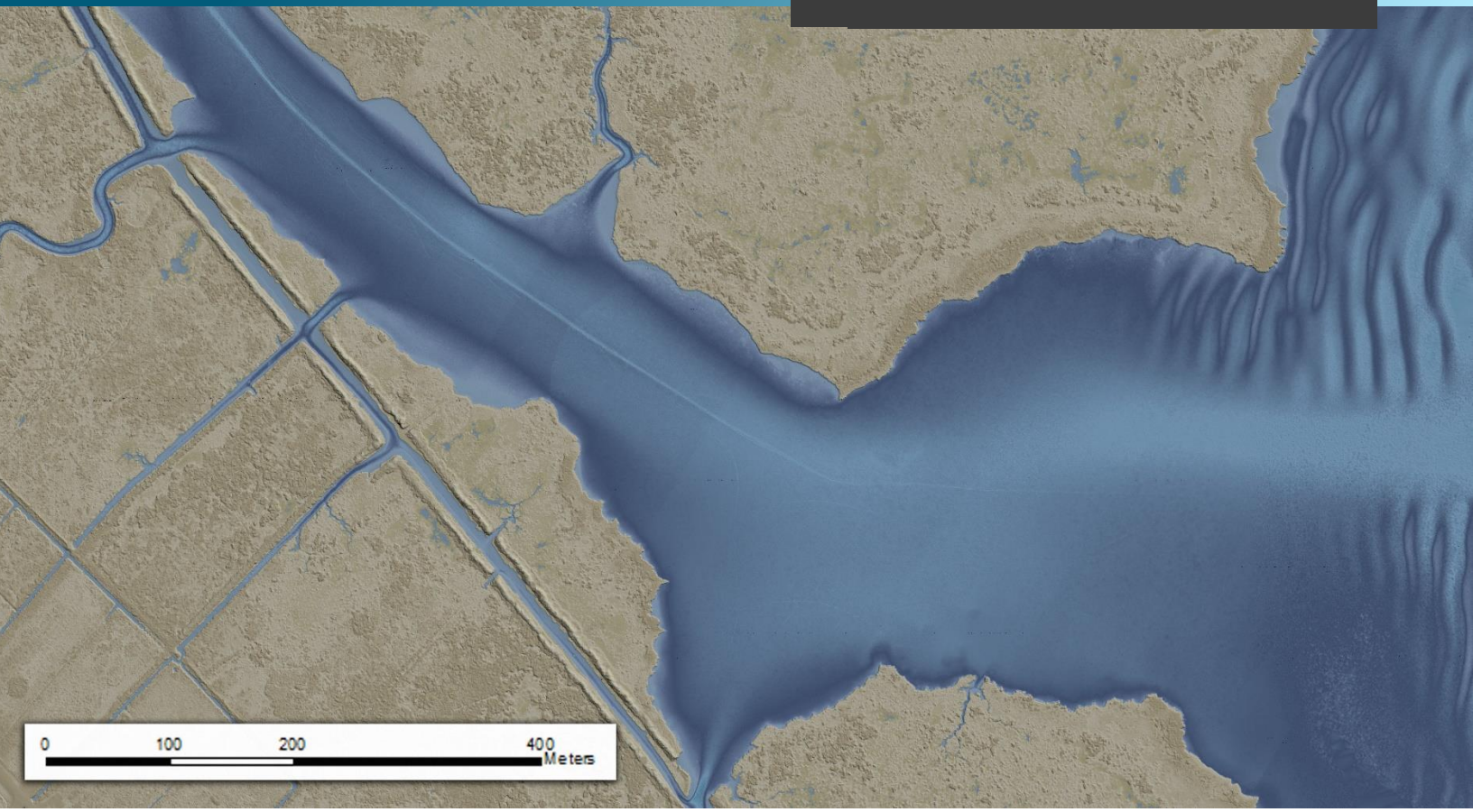

NOAA Hurricane Florence, North Carolina

Lidar, Digital Imagery & Shoreline Mapping: NC1901, NC1902, & NC1903-TB-C

Technical Data Report, NOAA Contract: EA-133C-14-CQ-0007

Prepared For:

NOAA; National Geodetic Survey
1315 East West Highway
Silver Spring, MD 20910
PH: 301-713-3167 ext.133

Prepared By:

NV5 GEOSPATIAL
powered by QUANTUM SPATIAL

NV5 Geospatial
1100 NE Circle Blvd, Ste. 126
Corvallis, OR 97330
PH: 301-713-3198

Table of Contents

Project Summary 1
Introduction 1
Survey Area 2
Project Team 3
Deliverable Products 3
LiDAR Deliverables 5
DEM Deliverables 5
Imagery Deliverables 7
Shoreline Deliverables 7
Acquisition 8
Sensor Selection 8
Riegl VQ-880-G Series 8
Leica Chiroptera Hawkeye CH4X 8
Logistics Planning 9
Turbidity & Tide Monitoring 9
Airborne LiDAR Surveys 11
Airborne Collection Logs & Coverage Reports 13
Ground Survey 14
Primary Control 14
Network Accuracy 17
Equipment and Collection Methods 18
Lidar Survey Point Collection 18
Lidar Point Positions 18
Digital Imagery 20
Aerial Targets 20
Data Processing 22
LiDAR Data Calibration 22
Bathymetric Refraction 23
Topobathymetric DEMs 26
Results & Discussion 27
LiDAR Point Density 27
LiDAR Accuracy Assessments 27

Lidar Non-Vegetated Vertical Accuracy (NVA) 27
Lidar Bathymetric Vertical Accuracies 35
Lidar Vegetated Vertical Accuracies 37
Lidar Relative Vertical Accuracy 39
Lidar Horizontal Accuracy 40
Digital Imagery Accuracy Assessment 40
Lessons Learned 40
GLOSSARY 41
APPENDIX A - ACCURACY CONTROLS 42
APPENDIX B - AT REPORT 1

Cover Photo: A nadir view of Middle Town Creek along the North Carolina coast. The image was created from the gridded topobathymetric bare earth model colored by elevation.

PROJECT SUMMARY

An aerial view of the NOAA Hurricane Florence project area, taken by NV5G's onboard sensor operator.

Introduction

In November 2019, NV5 Geospatial (powered by Quantum Spatial), was contracted by the National Oceanic and Atmospheric Administration's (NOAA) National Geodetic Survey (NGS) Remote Sensing Division (RSD) Coastal Mapping Program (CMP), to collect topobathymetric light detection and ranging (Lidar) data and digital imagery from November of 2019 through August of 2020 to support the development of shoreline feature mapping for the NOAA Hurricane Florence project site (Contract No. EA-133C-14-CQ-0007). The NOAA Hurricane Florence project area covers approximately 4,805 square miles and 6,511 shoreline miles along the eastern coast of the United States, beginning near Cape Henry, Virginia, and stretching south to Winyah Bay, South Carolina. Data were collected to assist NOAA in the accurate and consistent measurement of the national shoreline, and to support nautical charting, geodesy services, marine debris surveys, and marine resource management.

The topobathymetric LiDAR dataset was divided, processed, and delivered in nine separate deliveries, while shoreline mapping products were processed according to Geographic Cell delineations provided by NOAA. NV5 Geospatial provided all Digital Imagery in one delivery package. This report provides a comprehensive summary of the delivered topobathymetric LiDAR, digital imagery dataset, and shoreline compilation products. Documented herein are contract specifications, data acquisition procedures, processing methods, and accuracy results. Acquisition dates and acreage are shown in Table 1, a complete list of contracted deliverables provided to NOAA is shown in Table 2, and the project extent is shown in Figure 1.

Table 1: Acquisition dates, acreage, and data types collected for the NOAA Hurricane Florence project

Project Site	Contracted Acres	Square Miles	Acquisition Dates	Data Type
NOAA Hurricane Florence, North Carolina	3,075,010	4,805	11/26/2019 – 08/28/2020	Topobathymetric LiDAR
			01/05/2020 – 04/17/2020	4 Band Digital Imagery (RGB-NIR)

Survey Area

The NOAA Hurricane Florence project area was contracted to cover approximately 4,805 square miles along the eastern shorelines of the states of North Carolina, Virginia, and South Carolina. The project was divided into three sub-areas: NC-1901-TB-C, NC-1902-TB-C, and NC1903-TB-C (Figure 1). During the acquisition of the project, an additional area covering deeper waters within the Pamlico Sound in North Carolina was added to the project boundary to be collected with deep-channel sensor technology. NV5 Geospatial conducted all LiDAR acquisition of the main project area between November 26th, 2019 and May 30th, 2020. The Pamlico Sound "deep channel" dataset was collected between May 29th, 2020, and August 28th, 2020. All digital imagery acquisition for the Hurricane Florence project was conducted between January 5th, 2020 and April 17th, 2020, by NV5 Geospatial.

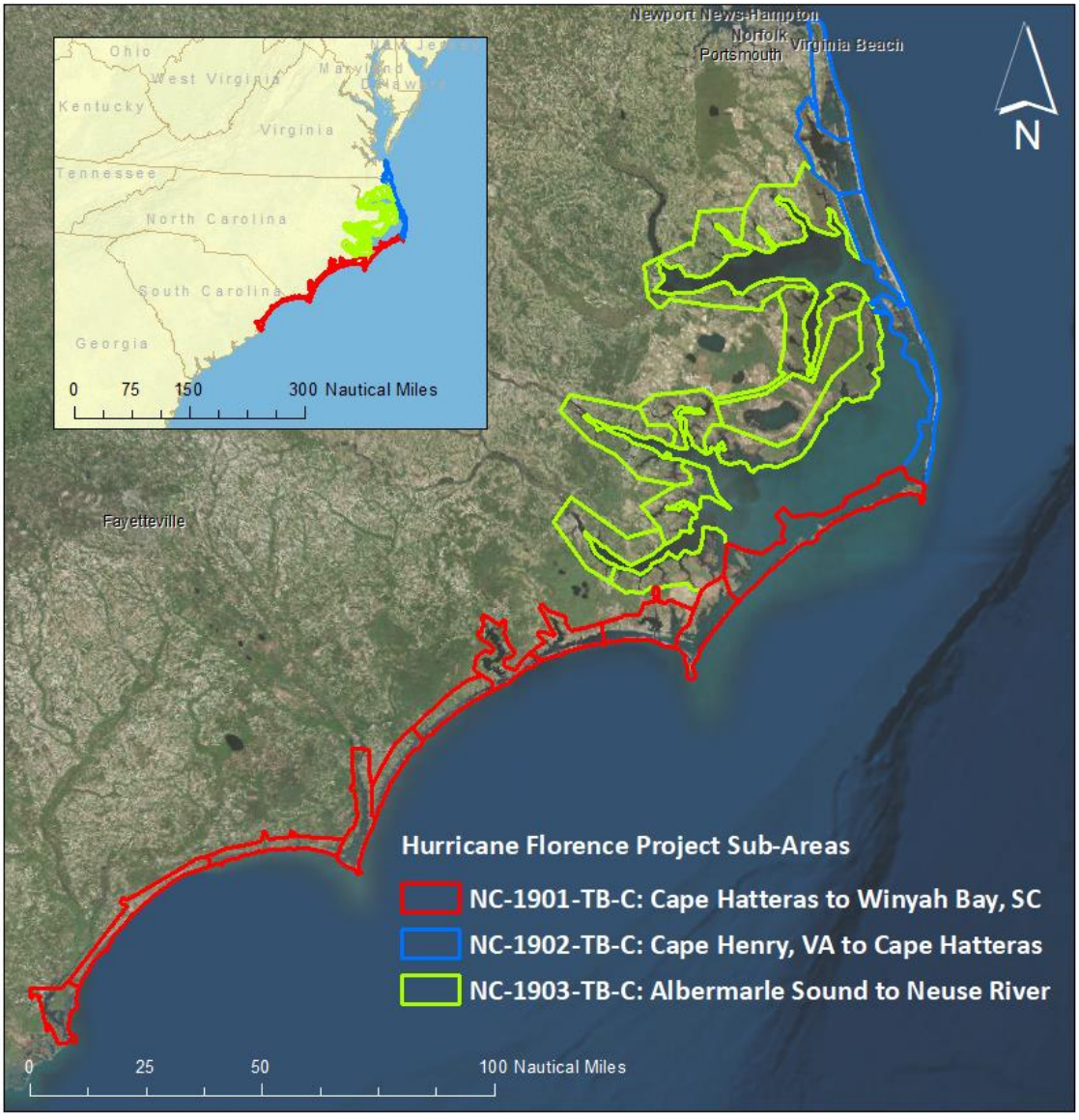

Figure 1: Location map of the NOAA Hurricane Florence project

Project Team

NV5 Geospatial served as the prime contractor for the Hurricane Florence project and completed all LiDAR processing including lidar extraction, calibration and refraction, and editing. NV5 Geospatial worked with Leading Edge to complete lidar acquisition of the Hurricane Florence project area. NV5 Geospatial generated all Digital Elevation Models (DEM), raster layers, and LiDAR-derived void polygons from processed LiDAR data. Additionally, NV5 Geospatial collected all independent checkpoints to be used in assessing vertical accuracy.

NV5 Geospatial conducted all digital imagery acquisition and processing. All ground survey collection to support the imagery production was completed by NV5 Geospatial's Lexington office.

NGS derived the initial shoreline files from the final delivered topobathymetric LiDAR data, and provided them to NV5 Geospatial for editing and attribution. All shoreline editing and deliverables were completed by NV5 Geospatial's St. Petersburg office, or with collaboration from Fugro.

Deliverable Products

Table 2: Products delivered to NOAA for the NOAA Hurricane Florence Supplemental topobathymetric lidar project

NOAA Hurricane Florence Topobathymetric LiDAR Products	
Classified LAS Projection: UTM Zone 18 North **Horizontal Datum: NAD83 (2011)** **Vertical Datum: GRS80 Ellipsoidal Heights** **Units: Meters**	**DEM Projection: UTM Zone 18 North** **Horizontal Datum: NAD83 (2011)** **Vertical Datum: NAVD88 (Geoid18)** **Units: Meters**
LiDAR	LAS v 1.4, Point Format 6 – Ellipsoidal & Orthometric Heights • All Classified Returns, with Depth Bias Correction for Depth
Raster Models	1.0 Meter GeoTIFF Files (*.tif) • Bathymetric Void Clipped Topobathymetric Bare Earth Digital Elevation Model (DEM) • Topobathymetric Standard Deviation Model • NIR Sensor DZ Orthos • Green Sensor DZ Orthos
TPU Deliverables	1.0 Meter ERDAS Imagine Files (*.img) • Total Propagated Uncertainty Raster Model cBLUE Products • LAS v 1.4, Point Format 6 with TPU Extrabyte (*.las) • TPU Metadata (*.json)

NOAA Hurricane Florence Topobathymetric LiDAR Products	
Digital Imagery	• 6 inch Tiled Orthomosaic GeoTiffs (*.tif) • Raw Image Frames with Socet Set SUP files and camera calibrations.
Shoreline Mapping	Shapefiles (*.shp) • Segmented Mean High Water Shoreline • Segmented Mean Lower Low Water Shoreline
Vectors	Shapefiles (*.shp) • Area of Interest • LiDAR Tile Index • DEM Tile Index • Bathymetric Void Shape • Flightline Shapefile • Flight Date Coverage Polygon

Reports	• Ground Survey Reporting
	  ○ *NOAA HurrFlorence PRELIMINARY Ground Survey Report for Lidar.pdf*
	  ○ *NOAA HurrFlorence PRELIMINARY Ground Survey Report for Imagery.pdf*
	• Check Point Location Photos
	  ○ *NC1901_NC1902_NC1903_photos_lidar.zip*
	  ○ *NC1901_NC1902_NC1903_photos_imagery.zip*
	• LiDAR QC Reports per Delivery
	• Final Compiled Report of Survey
	• FGDC Compliant Metadata
	• Airborne Collection Log and Lift Extents/Coverage
	• Airborne Navigation and Kinematic GPS Reports
	• Aerotriangulation Report (*NC1901_NC1902_NC1903_Hurricane_Florence_AT_Report_QSI.doc*)
	• Airborne Positioning and Orientation Reports
	• Boresight Calibration Report
	• Camera Calibration Reports
	• EED
	• Photographic Flight Reports & Flightline Maps
	• Tabulation of Aerial Photography
	• Shoreline Mapping Project Completion Reports

LiDAR Deliverables

Final topobathymetric LiDAR deliverables for the NOAA Hurricane Florence project area were the final classified and tiled LiDAR returns, DZ ortho raster models, Standard Deviation raster models, topobathymetric bare earth DEMs, and supplemental shapefiles including bathymetric void polygons and flightline swaths. NV5 Geospatial also provided several intermittent deliverables to NOAA to ensure project quality, consistency, and transparency in processing throughout the project. These additional intermittent deliverables included Quick-look LiDAR coverage maps in GeoTIFF format to display bathymetric LiDAR collection results. NOAA reviewed all QuickLook reports and approved each area for data processing or flagged each area to re-fly. RiProcess projects were also provided along with SBETs for each LiDAR collection mission to ensure that NOAA is provided with all raw topobathymetric data.

Final topobathymetric data was provided in 500 x 500-meter tiles and delivered in nine processing blocks (Figure 2). All associated shapefiles delineating tile grids were provided to NOAA in Blocks, and as a final comprehensive tile index for the NOAA Hurricane Florence project area. Final LiDAR DZ Orthos were created to evaluate the line to line relative accuracy of the LiDAR data, and were delivered to NOAA in GeoTIFF format. Project metadata in .xml format was delivered with all final LiDAR data and derived deliverables.

DEM Deliverables

After the final LiDAR data were accepted by NOAA, NV5 Geospatial processed the final classified point cloud into the contracted DEM deliverables. First, data were converted from ellipsoid heights to orthometric heights prior to DEM generation so that all final tiled DEMs include orthometric heights from Vertical Datum NAVD88, Geoid 18, meters.

NV5 Geospatial provided two sets of tiled DEMs to NOAA: one with void polygons enforced so that areas lacking bathymetric bottom returns are set to “no data”, and one with void areas interpolated. All DEMs were delivered in ERDAS Imagine (*.img) format with a 1 meter cell size, tiled in a 5,000 x 5,000 meter grid. Void polygons used in DEM generation were provided in addition to a confidence layer. The confidence layer reports the standard deviation (in meters) of all ground and bathymetric bottom return points within each 1 meter cell, provided in ERDAS Imagine (*.img) format with a 1 meter pixel resolution, tiled in 500 x 500 meter grid.

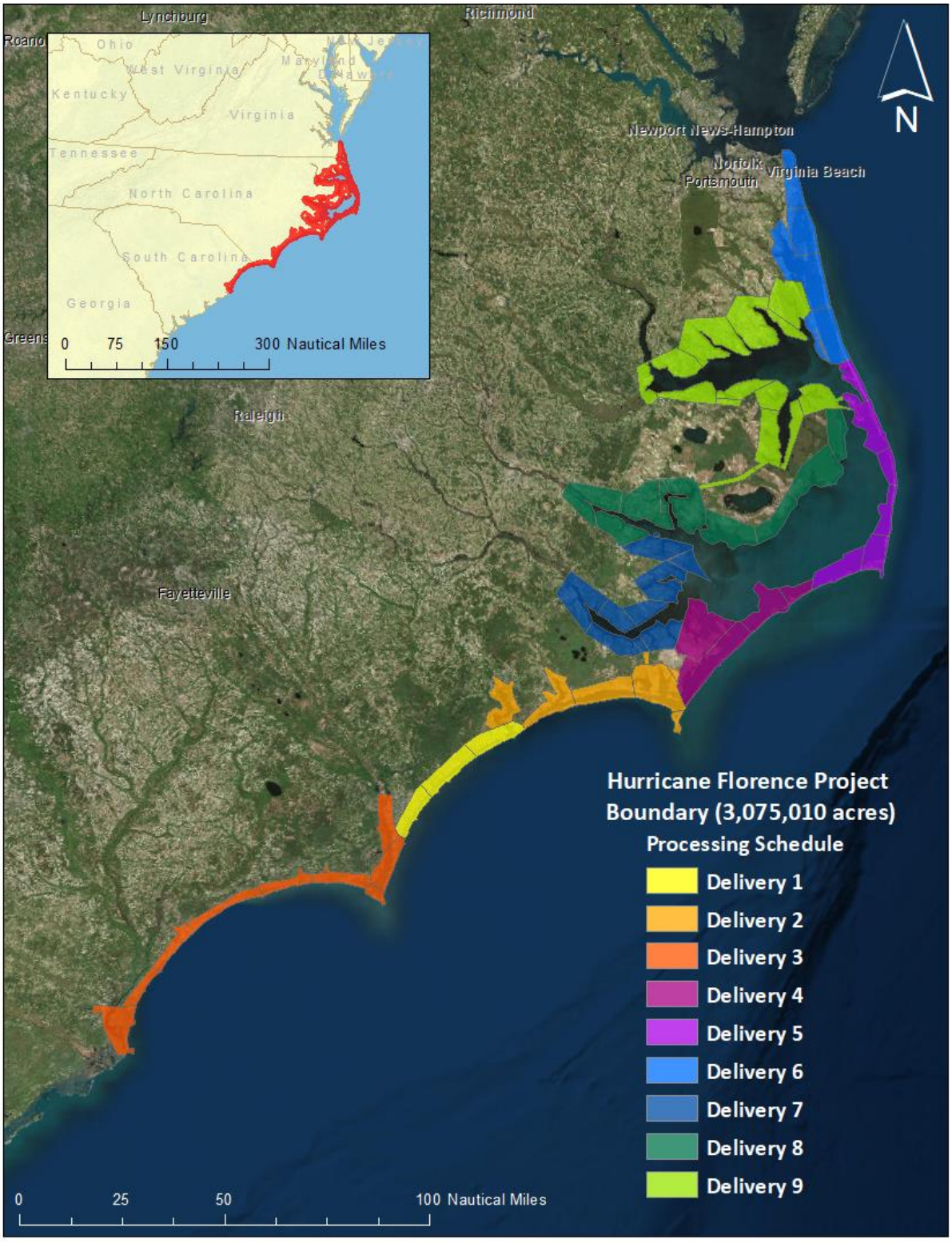

Figure 2: Lidar Delivery and Processing Blocks

Imagery Deliverables

NV5 Geospatial provided NOAA with all acquired image frames to be viewed in both stereo as well as mosaic format. All appropriate imagery orientation and calibration information was provided along with image frames, including Socet Set SUP files and a center point shapefile. Metadata were delivered in .xml format for both stereo imagery and orthomosaics.

The collected 4-band (RGB/NIR) digital imagery was processed with 3000 x 3000 meter tile delineation, and mosaicked in GeoTIFF format. Final orthomosaics were provided in the deliverable coordinate system: Projection: UTM Zone 18 North, Horizontal Datum: NAD83 (2011) epoch 2010.00, meters. For detailed processing information, please reference documentation provided with the imagery delivery, which includes: Aerotriangulation Report, Airborne Positioning and Orientation Report, Boresight Calibration Report, Camera Calibration Reports, EED, Flightline Maps, Ground Control Report, Photographic Flight Reports, and Tabulation of Aerial Photography.

Shoreline Deliverables

NOAA supplied NV5 Geospatial with LiDAR derived Mean High Water (MWH) and Mean Lower-Low Water (MLLW) shorelines to be segmented, edited, and attributed. In addition, NV5 Geospatial was responsible for compiling any shoreline features that were unable to be extracted from the LiDAR. These features were compiled photogrammetrically using stereo imagery flown specifically for this project.

NV5 Geospatial received and mapped the shoreline from NOAA in twenty-four (24) processing blocks, with each processing block identified with a Geographic Cell number and including all bays, inlets, and islands within 2000 feet of the coastline.

Successful completion of this project resulted in digital feature data of the coastal zone in support of the NOAA Nautical Charting Program (NCP) as well as geographic information systems (GIS) for a variety of coastal zone management applications. The project database consists of information measured and extracted from satellite photographs and metadata related to photogrammetric compilation. Base mapping was conducted in a digital environment using stereo softcopy photogrammetry and associated cartographic practices, supplemented with lidar derived Mean High Water (MHW) and Mean Lower Low Water (MLLW) data provided by NOAA.

Quality control tasks were conducted during all phases of project completion by an NV5 Geospatial senior mapping professional. The review process included analysis of aero-triangulation results and assessment of the identification and attribution of digital feature data within the subproject according to image analysis and criteria defined in C-COAST. The quality control process concluded with an inspection of topological connectivity within the project using ArcGIS 10.6 software. All project data was evaluated for compliance to CMP requirements.

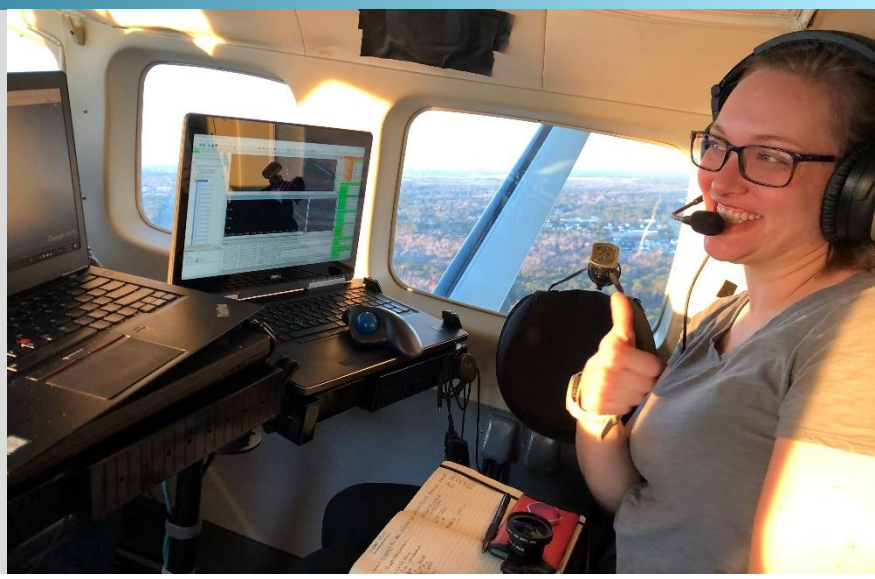

NV5G's sensor operator working on topobathymetric lidar collection for the NOAA Hurricane Florence project.

Sensor Selection

Riegl VQ-880-G Series

The Riegl VQ-880-G (Gii and G+) series were selected as the hydrographic airborne laser scanners for the NOAA Hurricane Florence project based on fulfillment of several considerations deemed necessary for effective mapping of the project site. A higher combined pulse rate (up to 550 kHz), higher scanning speed, small laser footprint, and wide field of view allow for seamless collection of high-resolution data of both topographic and bathymetric surfaces. A short laser pulse length allows for discrimination of underwater surface expression in shallow water.

Leica Chiroptera Hawkeye CH4X

NV5 Geospatial also selected the Leica Chiroptera 4X (CH4X) as a supplemental sensor system for the NOAA Hurricane Florence project, to be used in targeting the deeper channel areas within Pamlico Sound, North Carolina. The CH4X laser system was dually mounted with an additional Leica 40kHZ deep bathymetric channel known as a Leica HawkEye 4X (HE4X). The HE4X boasts a higher density point cloud in addition to excellent topographic, shallow water, and deep-water performance down to 50 m depth. Sensor specifications and settings for the NOAA Hurricane Florence acquisition are displayed in Table 3.

Logistics Planning

In preparation for data collection, NV5 Geospatial reviewed the project area and developed a specialized flight plan to ensure complete coverage of the NOAA Hurricane Florence LiDAR study area at the target point density of ≥4.0 points/m^2. Acquisition parameters including orientation relative to terrain, flight altitude, pulse rate, scan angle, and ground speed were adapted to optimize flight paths and flight times while meeting all contract specifications. NV5 Geospatial acquisition managers oversaw all logistical considerations including private property access and coordination of NOTAMs prior to flights.

Figure 3: NV5G's Semi-Portable YSI Water Quality Monitor set up at Albemarle Plantation Marina, NC.

Turbidity & Tide Monitoring

NV5 Geospatial's acquisition team considered several environmental conditions during the planning stage of the project to target the best possible windows for capturing bathymetric bottom returns. Water clarity was monitored on a daily basis using handheld Hach turbidity meters and semi-portable water quality data loggers operated by NV5 Geospatial ground operations professionals (Figure 3). Water quality was also continuously monitored using three water quality monitoring stations operated by the National Estuary Research Reserve (NERR), as shown in Figure 4.

Figure 4: NERR Water Quality Monitoring Stations Utilized for the Hurricane Florence project

Flights over shoreline areas were planned during optimal conditions with low wind and wave conditions whenever possible, and within 20% of the Mean Range of tide around Mean Lower Low Water (MLLW) as specified in the task order. NV5 Geospatial acquisition teams carefully monitored NOAA tide stations to ensure acquisition requirements were met or exceeded (Figure 5).[1]

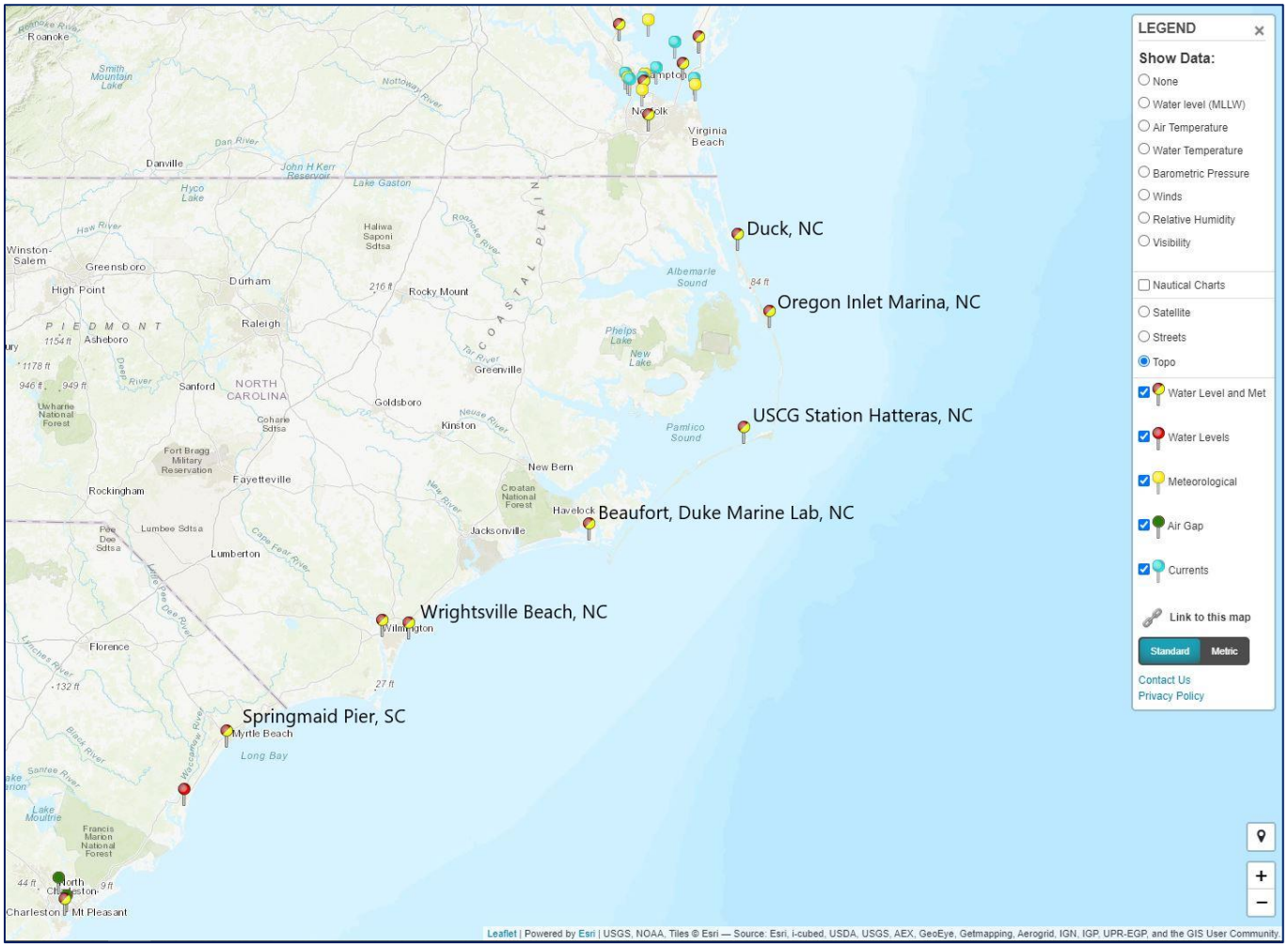

Figure 5: NOAA Tide Station Map

[1] NOAA Tides and Currents: https://tidesandcurrents.noaa.gov/map/

Airborne LiDAR Surveys

The LiDAR survey was accomplished using a Riegl VQ-880-GII, VQ-880-G+, or Leica Chiroptera 4X (CH4X) laser system dually mounted with an additional Leica 40kHZ deep bathymetric channel known as a Leica HawkEye 4X (HE4X). The HawkEye 4X (HE4X) boasts a higher density point cloud in addition to excellent topographic, shallow water, and deep-water performance. Both Riegl and Leica topobathymetric sensors utilize a green wavelength (ʎ=532 nm) laser capable of collecting high resolution vegetation and topography data, as well as penetrating the water surface with minimal spectral absorption by water. Both sensors also contain an integrated NIR laser (ʎ=1064 nm) that aids in water surface modeling for refraction purposes. The recorded waveform enables range measurements for all discernible targets for a given pulse. It is not uncommon for some types of surfaces (e.g., dense vegetation or water) to return fewer pulses to the LiDAR sensor than the laser originally emitted. The discrepancy between first return and overall delivered density will vary depending on terrain, land cover, and the prevalence of water bodies. All discernible laser returns were processed for the output dataset. Table 3 and Table 4 summarize the settings used to yield an average first return pulse density of ≥4 pulses/m^2 over the NOAA Hurricane Florence project area.

Table 3: Riegl Lidar Sensor specifications and survey settings

Riegl Survey Settings & Specifications		
Acquisition Dates	11/26/2019 – 05/30/2020	11/26/2019 – 05/30/2020
Aircraft Used	Cessna Caravan	Cessna Caravan
Sensor	Riegl	Riegl
Laser	VQ-880-GII/G+	VQ-880-GII/G+-IR
Maximum Returns	15 (LAS 1.4 Format)	15 (LAS 1.4 Format)
Resolution/Density	To exceed 4 pulses/m^2	To exceed 4 pulses/m^2
Nominal Pulse Spacing	0.50 m	0.50 m
Survey Altitude (AGL)	400 m	400 m
Survey speed	140 knots	140 knots
Field of View	40°	40°
Mirror Scan Rate	80 revolutions per second	Uniform Point Spacing
Target Pulse Rate	245 kHz	245 kHz
Pulse Length	1.5 ns	3 ns
Laser Pulse Footprint Diameter	28 cm	8 cm
Central Wavelength	532 nm	1064 nm
Pulse Mode	MTA (multiple times around)	MTA (multiple times around)
Beam Divergence	0.7 mrad	0.2 mrad
Swath Width	291 m	291 m
Swath Overlap	30%	30%
Intensity	16-bit	16-bit
Accuracy	$RMSE_Z \leq 15$ cm	$RMSE_Z \leq 15$ cm

Figure 6: Riegl VQ-880-ii Lidar sensor

Table 4: Chiroptera Lidar Sensor specification and survey settings

Chiroptera Survey Settings & Specifications			
Acquisition Dates	05/29/2020 – 08/28/2020	05/29/2020 – 08/28/2020	05/29/2020 – 08/28/2020
Aircraft Used	Cessna Caravan	Cessna Caravan	Cessna Caravan
Sensor	Leica	Leica	Leica
Laser	Chiroptera 4X (NIR)	Chiroptera 4X (shallow green)	HawkEye 4X (HE4X)
Maximum Returns	15	15	15
Resolution/Density	To exceed 8 pulses/m^2	To exceed 2 pulses/m^2	To exceed 2 pulses/m^2
Nominal Pulse Spacing	0.35 m	0.71 m	0.71 m
Survey Altitude (AGL)	400-600 m	400-600 m	400-600 m
Survey speed	130 knots	130 knots	130 knots
Field of View	40°	40°	40°
Mirror Scan Rate	70 Hz	32-39 Hz	17-21 Hz
Effective Target Pulse Rate	300-450 kHz	140 kHZ	40 kHz
Pulse Length	2.5 ns	2.5 ns	2.5 ns
Laser Pulse Footprint Diameter	88-132 cm	88-132 cm	88-132 cm
Central Wavelength	1064 nm	532 nm	532 nm
Pulse Mode	Continuous multipulse	Continuous multipulse	Continuous multipulse
Beam Divergence	0.25 mrad	0.25 mrad	0.25 mrad
Swath Width	291-437 m	291-437 m	291-437 m
Swath Overlap	15%	20%	20%
Intensity	16-bit	16-bit	16-bit
Accuracy	$RMSE_Z \leq 15$ cm	$RMSE_Z \leq 15$ cm	$RMSE_Z \leq 15$ cm

Figure 7: Leica Chiroptera CH4X and HawkEye HE4X Lidar Sensor System

All areas were surveyed with an opposing flight line side-lap of ≥30% (≥60% overlap) in order to reduce laser shadowing and increase surface laser painting. To accurately solve for laser point position (geographic coordinates x, y and z), the positional coordinates of the airborne sensor and the attitude of the aircraft were recorded continuously throughout the LiDAR data collection mission. Position of the aircraft was measured twice per second (2 Hz) by an onboard differential GPS unit, and aircraft attitude was measured 200 times per second (200 Hz) as pitch, roll and yaw (heading) from an onboard inertial measurement unit (IMU). To allow for post-processing correction and calibration, aircraft and sensor position and attitude data are indexed by GPS time.

Airborne Collection Logs & Coverage Reports

NV5 Geospatial provided daily airborne collection logs to NOAA throughout the acquisition process in the form of a daily blog and acquisition tracker update on NV5 Geospatial's tracking platform Q-AURA (QSI Acquisition Update & Review Application, Figure 8). Information included in each report detailed the collection date, tide window and conditions, lines collected, coverage, and operator notes.

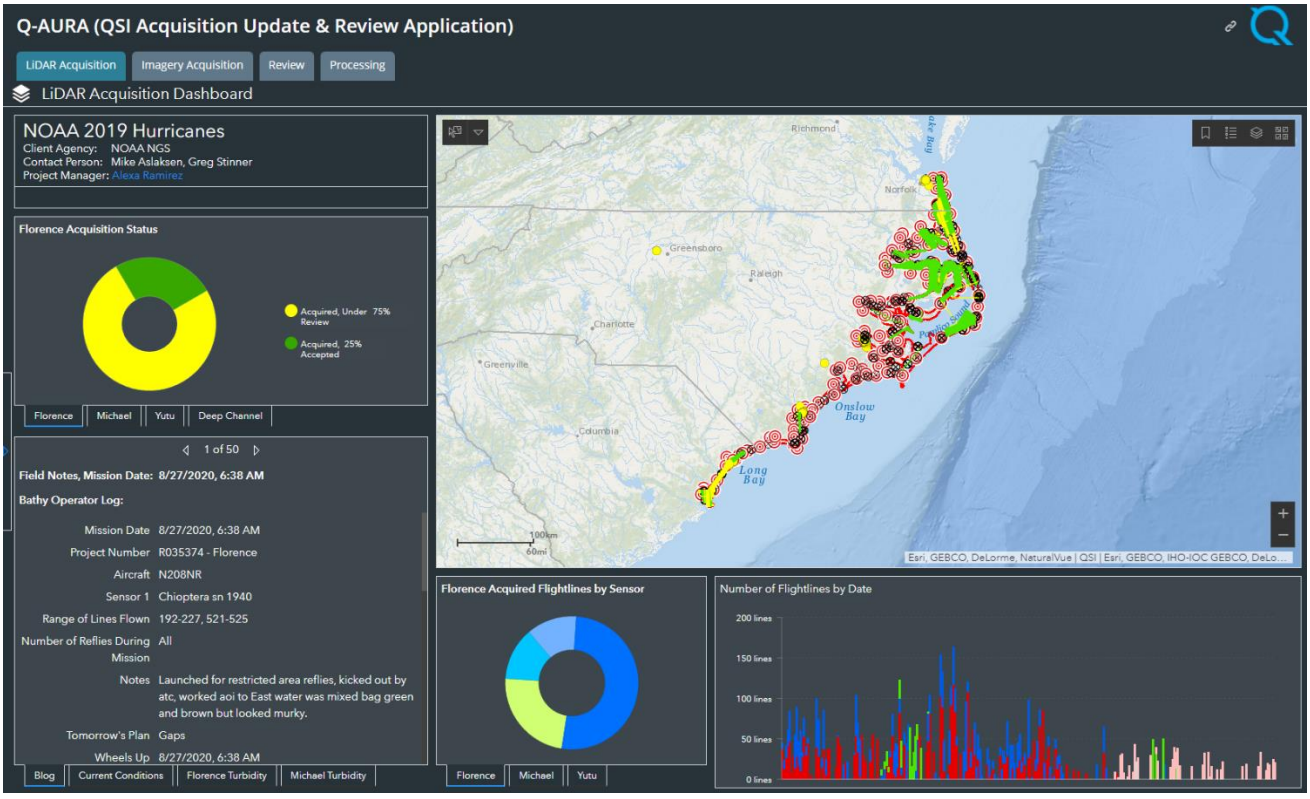

Figure 8: A sample image of the Q-AURA interface

Ground Survey

Ground control surveys including primary control stations, control points, and check points were conducted to support the airborne acquisition. This section summarizes the ground survey results including network stations utilized for this project, overall network accuracy, equipment used, and point tables for both the horizontal and vertical control points and check points – collectively, ground survey points (GSPs).

Primary Control

NV5 Geospatial utilized 34 permanent real-time network (RTN) stations for the NOAA Hurricane Florence project. Twelve base stations were from the Hexagon SmartNet[2] network, 18 base stations were from the North Carolina DOT[3] network, three base stations were from the South Carolina RTN[4], and one base station was from the KeyNetGPS RTN[5]. Record positions were held for all base stations.

No physical monuments were utilized for this project.

The position, precision, and network of each primary control station have been provided in Table 5 and Table 6. Precision values shown are for the 68% (1-sigma) confidence interval. Units are in meters unless specified otherwise. Horizontal coordinates are in the UTM18 projection and referenced to the NAD83(2011) reference frame, epoch 2010.00. Ellipsoid heights are relative to the GRS80 ellipsoid. Orthometric heights are derived using NGS Geoid18.

Table 5: Geodetic coordinates and status of primary control stations utilized for the NOAA Hurricane Florence acquisition.

Station ID	Latitude	Longitude	Ellipsoid Height	σ X	σ Y	σ Z	Network	Held?
LS03	36° 47' 19.43643"	-75° 57' 34.32963"	-22.039	n/a	n/a	n/a	SMARTNET	YES
NCBE	34° 43' 08.50895"	-76° 40' 18.99140"	-27.858	n/a	n/a	n/a	NCDOT	YES
NCBI	35° 50' 44.35730"	-75° 33' 48.94199"	-33.046	n/a	n/a	n/a	NCDOT	YES
NCBL	35° 33' 39.01838"	-76° 33' 57.78557"	-28.891	n/a	n/a	n/a	SMARTNET	YES
NCBX	35° 15' 58.08195"	-75° 33' 06.82901"	-25.451	n/a	n/a	n/a	NCDOT	YES
NCCH	34° 20' 40.22860"	-77° 52' 29.89892"	-22.806	n/a	n/a	n/a	NCDOT	YES
NCCI	35° 01' 03.76013"	-76° 18' 55.28490"	-30.613	n/a	n/a	n/a	NCDOT	YES
NCCM	35° 53' 19.25587"	-76° 13' 52.29683"	-29.665	n/a	n/a	n/a	SMARTNET	YES

[2] https://hxgnsmartnet.com/

[3] http://rtn.nc.gov/

[4] https://scgsrtn.sc.gov/SCGSRTN/

[5] https://www.keynetgps.com/

Station ID	Latitude	Longitude	Ellipsoid Height	σ X	σ Y	σ Z	Network	Held?
NCCR	35° 54' 56.93094"	-76° 28' 25.29184"	-28.218	n/a	n/a	n/a	NCDOT	YES
NCCU	36° 23' 46.05854"	-75° 59' 03.44572"	-27.497	n/a	n/a	n/a	SMARTNET	YES
NCDU	36° 10' 54.01098"	-75° 45' 04.79522"	-24.775	n/a	n/a	n/a	NCDOT	YES
NCEL	36° 20' 28.79075"	-76° 15' 29.27386"	-29.750	n/a	n/a	n/a	NCDOT	YES
NCEN	35° 30' 35.43309"	-76° 00' 48.05768"	-31.966	n/a	n/a	n/a	SMARTNET	YES
NCFF	33° 57' 38.26113"	-77° 56' 18.76581"	-29.165	n/a	n/a	n/a	NCDOT	YES
NCGA	36° 26' 12.65519"	-76° 43' 16.51667"	-20.469	n/a	n/a	n/a	NCDOT	YES
NCJK	34° 47' 34.75845"	-77° 22' 19.47145"	-18.582	n/a	n/a	n/a	SMARTNET	YES
NCJV	34° 44' 46.81575"	-77° 27' 11.71789"	-26.125	n/a	n/a	n/a	NCDOT	YES
NCKH	36° 02' 49.23740"	-75° 40' 55.11834"	-28.989	n/a	n/a	n/a	SMARTNET	YES
NCNB	35° 06' 45.99769"	-77° 06' 14.29783"	-16.105	n/a	n/a	n/a	NCDOT	YES
NCNR	35° 05' 18.78580"	-77° 02' 02.75292"	-27.430	n/a	n/a	n/a	SMARTNET	YES
NCNT	34° 44' 51.43959"	-76° 48' 30.82086"	-26.943	n/a	n/a	n/a	SMARTNET	YES
NCOI	35° 47' 43.59527"	-75° 32' 58.18063"	-34.800	n/a	n/a	n/a	NCDOT	YES
NCRT	35° 35' 43.43934"	-75° 28' 09.74394"	-31.520	n/a	n/a	n/a	NCDOT	YES
NCSL	33° 58' 57.20129"	-78° 23' 24.30664"	-10.002	n/a	n/a	n/a	NCDOT	YES
NCSO_NC*	35° 23' 40.93840"	-76° 19' 31.76848"	-29.918	n/a	n/a	n/a	NCDOT	YES
NCSO_SC*	33° 55' 42.04977"	-78° 04' 24.65306"	-22.669	n/a	n/a	n/a	SMARTNET	YES
NCWA	35° 33' 34.78457"	-77° 03' 31.44224"	-25.354	n/a	n/a	n/a	NCDOT	YES
NCWG	34° 19' 44.80539"	-77° 54' 27.59295"	-21.403	n/a	n/a	n/a	SMARTNET	YES
NCWM	35° 49' 49.75733"	-77° 02' 06.20978"	-21.891	n/a	n/a	n/a	NCDOT	YES
NCWN	35° 32' 34.90821"	-77° 24' 26.67037"	-7.797	n/a	n/a	n/a	SMARTNET	YES
SCGN	33° 23' 10.24077"	-79° 17' 26.74211"	-21.866	n/a	n/a	n/a	SCRTN	YES
SCHG	33° 47' 47.19678"	-79° 00' 12.54582"	-10.490	n/a	n/a	n/a	SCRTN	YES
SCHY	33° 56' 23.73653"	-78° 44' 06.88298"	-16.037	n/a	n/a	n/a	SCRTN	YES
WLP2	36° 45' 59.76802"	-76° 15' 30.56736"	-13.211	n/a	n/a	n/a	KEYNET	YES

* NCDOT and SCRTN independently include a station named NCSO. It is not a duplicate.

Table 6: UTM coordinates and orthometric heights of primary control stations utilized for the NOAA Hurricane Florence acquisition.

Station ID	Northing	Easting	Orthometric Height	σ X	σ Y	σ Z	Network	Held?
LS03	4071865.518	414387.491	15.885	n/a	n/a	n/a	SMARTNET	YES
NCBE	3843157.747	346905.152	9.636	n/a	n/a	n/a	NCDOT	YES
NCBI	3966976.123	449105.468	5.918	n/a	n/a	n/a	NCDOT	YES
NCBL	3936369.002	358071.337	8.353	n/a	n/a	n/a	SMARTNET	YES
NCBX	3902696.540	449801.832	13.269	n/a	n/a	n/a	NCDOT	YES
NCCH	3804100.556	235538.533	13.886	n/a	n/a	n/a	NCDOT	YES
NCCI	3875797.704	379993.743	7.224	n/a	n/a	n/a	NCDOT	YES
NCCM	3972301.753	388877.016	8.343	n/a	n/a	n/a	SMARTNET	YES
NCCR	3975614.282	367033.993	8.901	n/a	n/a	n/a	NCDOT	YES
NCCU	4028336.126	411732.718	10.835	n/a	n/a	n/a	SMARTNET	YES
NCDU	4004360.101	432439.292	14.106	n/a	n/a	n/a	NCDOT	YES
NCEL	4022542.759	387095.513	7.586	n/a	n/a	n/a	NCDOT	YES
NCEN	3930057.087	408105.846	6.670	n/a	n/a	n/a	SMARTNET	YES
NCFF	3761682.386	228461.411	8.302	n/a	n/a	n/a	NCDOT	YES
NCGA	4033779.753	345720.609	15.639	n/a	n/a	n/a	NCDOT	YES
NCJK	3852650.953	282978.668	18.486	n/a	n/a	n/a	SMARTNET	YES
NCJV	3847654.690	275423.538	10.942	n/a	n/a	n/a	NCDOT	YES
NCKH	3989377.748	438571.056	9.988	n/a	n/a	n/a	SMARTNET	YES
NCNB	3887575.220	308258.197	21.046	n/a	n/a	n/a	NCDOT	YES
NCNR	3884755.737	314572.055	9.851	n/a	n/a	n/a	SMARTNET	YES
NCNT	3846545.394	334450.957	10.519	n/a	n/a	n/a	SMARTNET	YES
NCOI	3961399.757	450347.533	4.134	n/a	n/a	n/a	NCDOT	YES
NCRT	3939175.265	457481.316	7.290	n/a	n/a	n/a	NCDOT	YES
NCSL	3765404.434	186799.921	25.762	n/a	n/a	n/a	NCDOT	YES
NCSO_NC*	3917622.341	379626.850	7.985	n/a	n/a	n/a	NCDOT	YES
NCSO_SC*	3758467.217	215877.724	14.352	n/a	n/a	n/a	SMARTNET	YES
NCWA	3937060.338	313412.097	11.252	n/a	n/a	n/a	NCDOT	YES
NCWG	3802478.370	232481.334	15.197	n/a	n/a	n/a	SMARTNET	YES

Station ID	Northing	Easting	Orthometric Height	σ X	σ Y	σ Z	Network	Held?
NCWM	3967058.840	316181.054	14.159	n/a	n/a	n/a	NCDOT	YES
NCWN	3935931.934	281760.177	28.141	n/a	n/a	n/a	SMARTNET	YES
SCGN	3702335.049	100781.985	12.661	n/a	n/a	n/a	SCRTN	YES
SCHG	3746797.632	129291.489	23.755	n/a	n/a	n/a	SCRTN	YES
SCHY	3761784.328	154722.791	18.773	n/a	n/a	n/a	SCRTN	YES
WLP2	4069719.717	387680.520	24.017	n/a	n/a	n/a	KEYNET	YES

* NCDOT and SCRTN independently include a station named NCSO. It is not a duplicate.

All four RTNs were evaluated and found to be in close alignment with the NSRS on the NAD83(2011) reference frame. No additional static GNSS processing in OPUS Projects was deemed necessary.

Network Accuracy

Base station coordinates were established or evaluated according to the national standard for geodetic control networks, as specified in the Federal Geographic Data Committee (FGDC) Geospatial Positioning Accuracy Standards for geodetic networks.[6] This standard provides guidelines for classification of monument quality at the 95% confidence interval as a basis for comparing the quality of one control network to another. The monument rating for this project is shown in Table 7.

Table 7: FGDC monument rating for network accuracy

Direction	Rating
1.96 * St Dev $_{NE}$:	0.020 m
1.96 * St Dev $_{z}$:	0.050 m

[6] Federal Geographic Data Committee, Geospatial Positioning Accuracy Standards (FGDC-STD-007.2-1998). Part 2: Standards for Geodetic Networks, Table 2.1, page 2-3. http://www.fgdc.gov/standards/projects/FGDC-standards-projects/accuracy/part2/chapter2

Equipment and Collection Methods

The RTK, PPK, and TS survey techniques were utilized for the ground survey as described previously in this report. NV5 Geospatial equipment used for the ground survey is summarized in Table 8.

Table 8: Equipment identification table. Does not include CORS antennas.

Receiver Model	Antenna	OPUS Antenna ID	Serial Numbers	Use
Trimble R8 Model 2	Integrated Antenna	TRMR8_GNSS	8595	Rover
Trimble R8 Model 3	Integrated Antenna	TRMR8_GNSS3	0435	Rover
Trimble R10	Integrated Antenna	TRMR10	8783, 9602	Rover
Nikon NPL-322+ 5” P Total Station		n/a	n/a	VVA
Trimble M3 Total Station		n/a	n/a	VVA

Lidar Survey Point Collection

A total of 11,509 GSPs were collected for the NOAA Hurricane Florence lidar project. Of these, 9,835 points were utilized as control during lidar processing, while 1,674 were withheld from processing for vertical accuracy checks – 169 for NVA, 123 for VVA, and 1,382 for bathymetric accuracy.

Horizontal reference points were not collected or utilized for lidar processing.

Lidar Point Positions

Due to the significant amount of GSPs collected, all lidar survey point positions and quality information are presented in an ESRI shapefile entitled “NC1901_NC1902_NC1903_ground_survey_lidar.shp”, which has been included with this report for reference and includes both control points and check points for lidar, see Figure 9. Horizontal coordinates listed in the shapefile are in the UTM18 projection and referenced to the NAD83(2011) reference frame, epoch 2010.00. Ellipsoid heights are relative to the GRS80 ellipsoid. Orthometric heights are derived using NGS Geoid18.

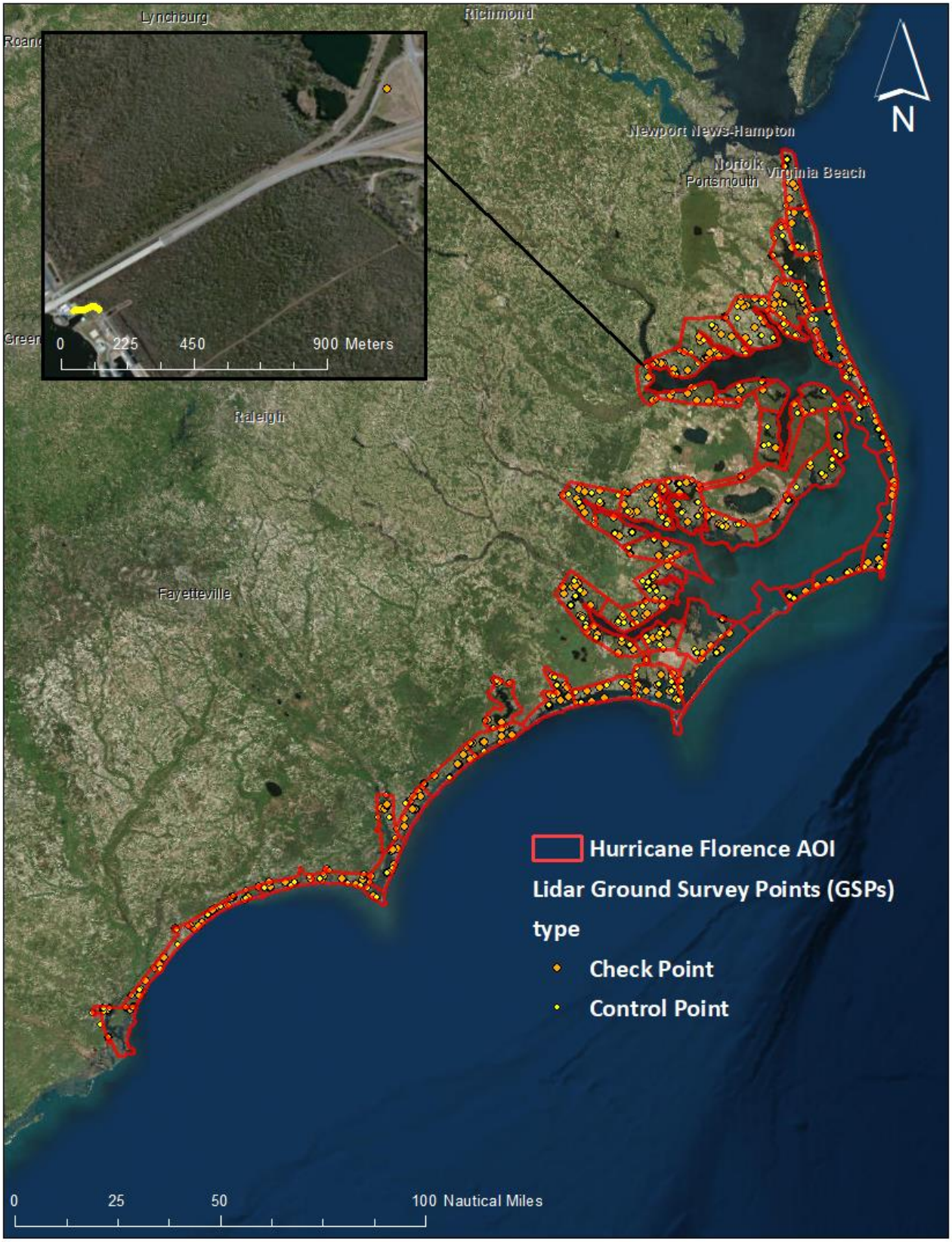

Figure 9: Lidar ground survey location map

Digital Imagery

Aerial imagery was collected by was flown by NV5 Geospatial and consisted of one hundred and one (101) flight lines. The photographs were acquired at a nominal ground sample distance of 0.33 meters using the Leica ADS100 push broom sensor. The 4band color photographs were acquired by NV5 Geospatial between January 5th, 2020 and April 17th, 2020. All imagery was acquired using >30% side overlap, sun angles >20 or >25 degrees (depending on the date of acquisition). The layout of the photographs is shown in Figure 10 and Figure 11. Photographic coverage, resolution, overlap, and metric quality were adequate for the performance of the aerotriangulation phase. Additional information can be found in the NC1901 \ NC1902 \ NC1903 Acquisition Summary report.

Aerial Targets

NV5 Geospatial conducted ground survey of one hundred thirteen (113) photo ID control points (horizontal and vertical), and 5 check points. Five surveyed points were used to check the horizontal and vertical accuracy of the aerotriangulation. A detailed report of survey for imagery was provided to NOAA in previous delivery packages.

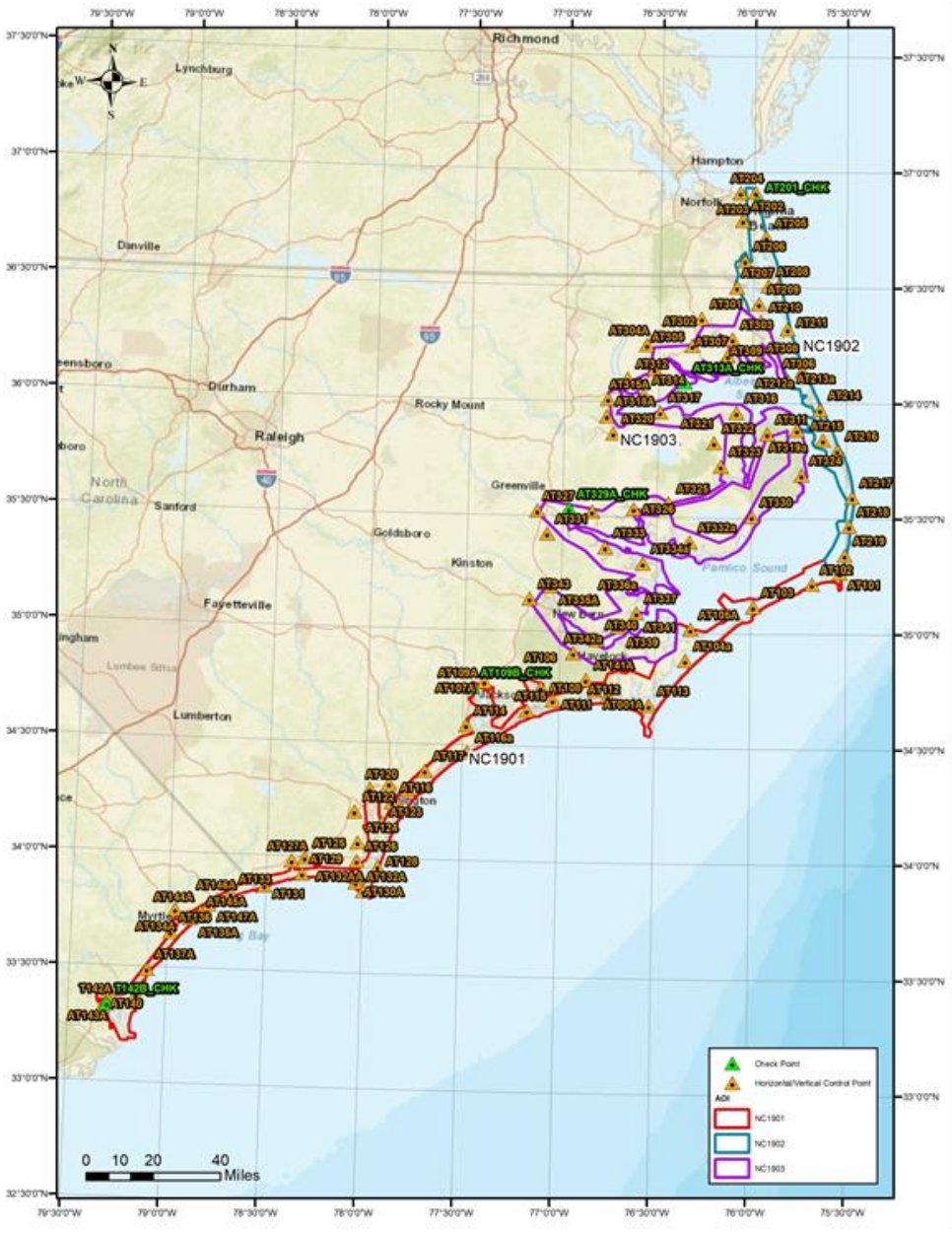

Figure 10: Imagery ground survey location map

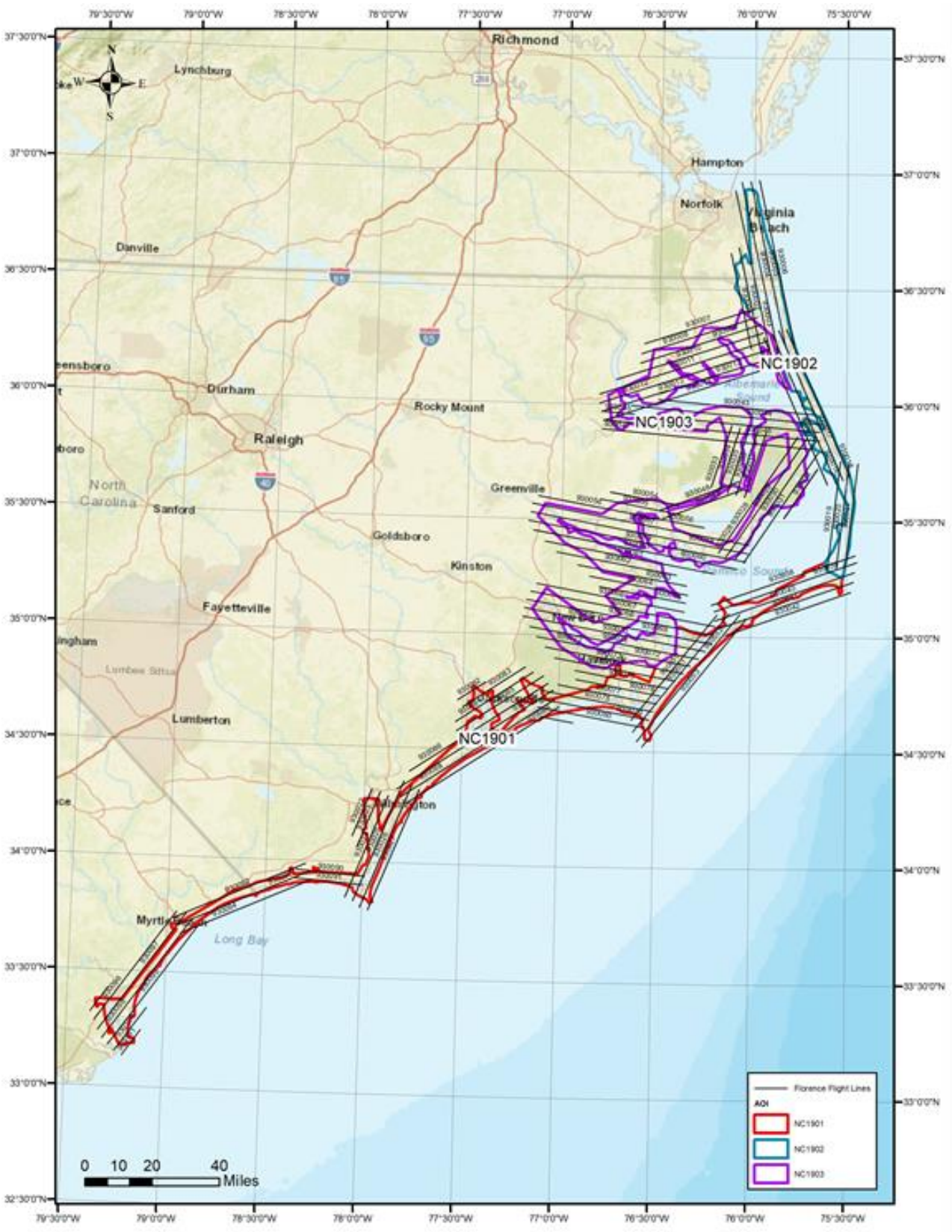

Figure 11: Map showing Hurricane Florence Imagery acquisition lines

LiDAR Data Calibration

Upon arrival of data in-house, NV5 Geospatial processing staff initiated a suite of automated and manual techniques to process the data into a geo-referenced point cloud ready for refraction processing and classification routines. Solutions for Smoothed Best Estimates of Trajectory (SBET) were processed using either Applanix POSPac 8.3 SP3 (with their Trimble® CenterPoint™ Post-Processed Real-Time Extended (PP-RTX) solution) or Novatel Inertial Explorer v.9 (with Terrastart NRT Precise Point Positioning (PPP) solution). This process utilizes the GPS and IMU data recorded onboard the aircraft, real-time data from a global reference station infrastructure, and advanced positioning and compression algorithms to calculate a highly accurate SBET for each mission.

Laser return point position computations were completed in Riegl's SDCImport and RiWorld software using the SBET and raw range information. After extracting the laser swaths, swath-to-swath geometric corrections were found using least square fit regression of matching tie plane objects in RiProcess. Individual lifts were adjusted to match vertical ground control points where available, and then integrated with corresponding overlapping lifts. Any remaining swath-swath discrepancies were further resolved using Terrasolid's TerraMatch application.

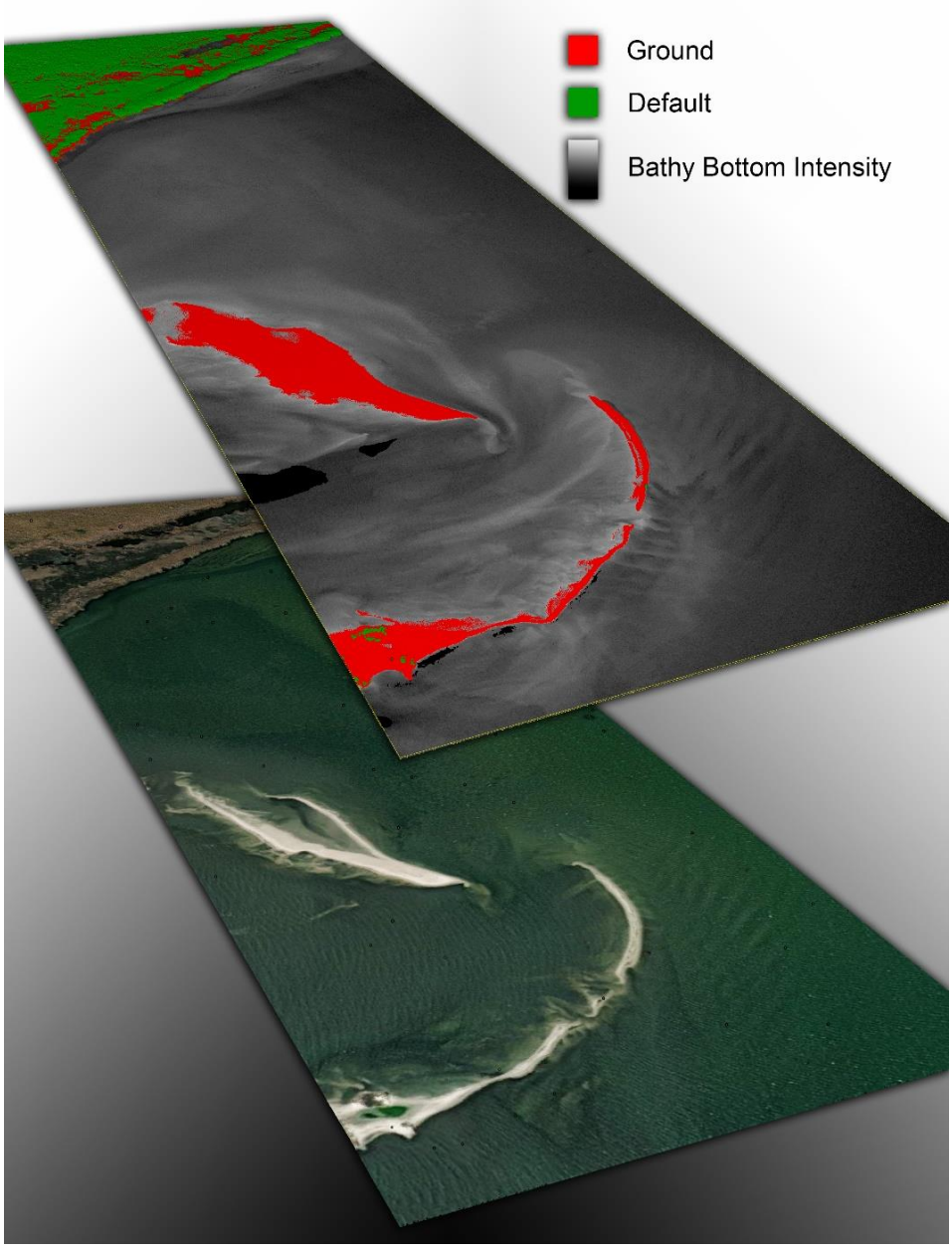

Figure 12: A 3D view of the lidar point cloud; the top layer is colored by class and intensity value, and the bottom later is colored by NAIP imagery.

Bathymetric Refraction

Following final SBET creation for the Leica Chiroptera 4X and Hawkeye systems, NV5 Geospatial used Leica Lidar Survey Studio (LSS) to calculate laser point positioning by associating SBET positions to each laser point return time, scan angle, and intensity. Leica LSS was used to derive a synthetic water surface to create a water surface model. Light travels at different speeds in air versus water and its direction of travel or angle is changed or refracted when entering the water column. The refraction tool corrects for this difference by adjusting the depth (distance traveled) and horizontal positioning (change of angle/direction) of the lidar data. All lidar data below the water surface model were classified as water column to correct for refraction. LSS then outputs the Lidar point cloud as classified LAS 1.4 files.

The water surface models used for refraction of Riegl sensor data were generated using elevation information from the point cloud. Where possible, points from the NIR channel were preferred due to the clean characteristics of water surface returns from that wavelength. However, because the NIR and green channels are not spatially and temporally coincident in the VQ-880-G system, where substantial wave action was present the green channels were used instead. Advanced classification routines were employed to ensure above-surface spray and below-surface backscatter points were not included in the model. Points were automatically classified, passed through filters appropriate to surface characteristics, and then manually edited to obtain the most accurate representation of the water surface. Models were created for each flight line to accommodate water level changes due to tide or other temporal factors.

The refraction correction was applied to submerged Riegl sensor returns using NV5 Geospatial's proprietary software Las Monkey. Points were flagged to refract based on their position relative to the triangulated irregular network model representing the water surface. Using the information from the trajectory and water surface model, each point was spatially corrected for refraction through the water column based on the angle of incidence of the laser to the model. The resulting point cloud was classified into its initial refracted scheme using automated techniques (Table 9).

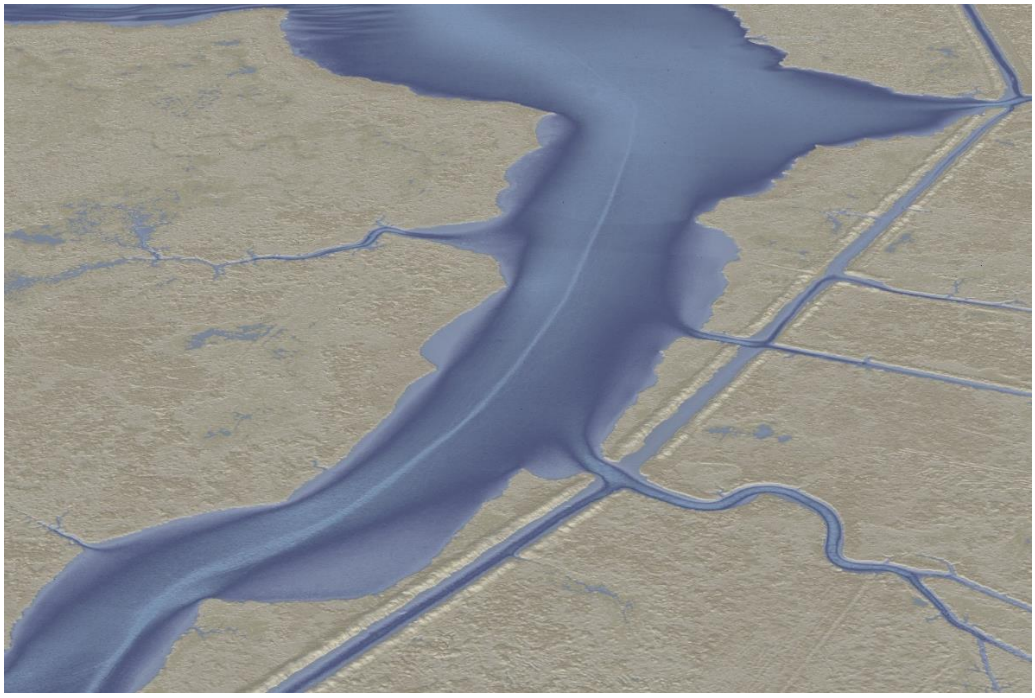

Figure 13: A view of Middle Town Creek along the North Carolina coast, created from the gridded topobathymetric bare earth model colored by elevation.

Table 9: ASPRS LAS classification standards applied to the NOAA Hurricane Florence dataset

Classification Number	Classification Name	Classification Description
1	Unclassified	Processed, but unclassified
2	Ground	Bare-earth ground
7	Noise	Noise (low or high; manually identified)
40	Bathymetric Bottom	Bathymetric point (e.g., seafloor or riverbed; also known as submerged topography)
41	Water Surface	Water's surface (sea/river/lake surface from topographic-bathymetric lidar
42- Synthetic	Derived Water Surface	Synthetic water surface location used in computing refraction at water surface
43	Submerged Feature	Submerged object, not otherwise specified (e.g., wreck, rock, submerged piling)
44	S-57 Object	International Hydrographic Organization (IHO) S-57 object, not otherwise specified
45	Water Column	Refracted returns not determined to be water surface or bathymetric bottom
46	Overlap Bathymetric Bottom	Denotes bathymetric bottom temporal changes from varying lifts, not utilized in the bathymetric point class
71	Adjacent Lift Unclassified	Adjacent lift Unclassified associated with areas of overlap bathy bottom where temporal bathymetric differences are present
72	Adjacent Lift Ground	Adjacent lift Ground associated with areas of overlap bathy bottom where temporal bathymetric differences are present
81	Adjacent Lift Water Surface	Adjacent lift Water Surface associated with areas of overlap bathy bottom where temporal bathymetric differences are present
81-Synthetic	Adjacent Lift Derived Water Surface	Adjacent lift Synthetic derived water surface associated with areas of overlap bathy bottom where temporal bathymetric differences are present
85	Adjacent Lift Water Column	Adjacent lift Water Column associated with areas of overlap bathy bottom where temporal bathymetric differences are present
1-Overlap	Edge Clip	Unclassified points flagged as withheld. These are primarily "edge" points from the higher scan angle being removed
1-Withheld	Unrefracted Green Chiroptera Points	Unrefracted green data from the Chiroptera 4X system
139	Withheld Tail Clip	These are points from the start/end of lines overlapping in adjoining lifts where flight data is not consistent or necessary to create coverage

Original SOW classification scheme	Delivered in LAS files
Additional classification codes	Delivered in LAS files
Original SOW classification code not used	Not delivered in LAS files
Deleted points	Not delivered in LAS files

Table 10: Lidar Processing Workflow

LiDAR Processing Step	Software Used
GNSS/IMU processing to create smoothed best estimate of trajectory using PP-RTX technology.	Applanix POSPac v.8.3 Service Pack 3 Novatel Inertial Explorer v.9 TerraStar NRT
Extract raw laser data and calculate laser point positions. Calculation combines raw ranging information, processed SBET, automated determination of MTA (Multiple-Time-Around) zone, and coordinate system information to extract and georeference each laser return.	Riegl SDCImport v.2.3 Riegl RiWorld v.5.1 Leica Lidar Survey Studio v.3
Sensor boresight. Per-lift geometric adjustments based on least-squares adjustment of feature matched tie planes.	Riegl RiProcess v.1.8
Apply refraction correction and depth bias correction to subsurface returns.	LAS Monkey v.2.0 (NV5 GEOSPATIAL) Leica Lidar Survey Studio v.3
Import raw laser points into manageable blocks to perform manual relative accuracy calibration and filter erroneous points. Classify ground points for individual flight lines.	TerraScan v.19
Using ground classified points per flight line, perform automated line-to-line calibrations for system attitude parameters (pitch, roll, and heading). Match data to vertical control points. Assess relative accuracies between overlapping lifts and relative within each lift and swath.	TerraMatch v.19 Las Product Creator v.3.4 (NV5 GEOSPATIAL)
Classify resulting data to ground and other client-designated classifications using manual and automated processes (Table 9). Assess statistical absolute accuracy via direct comparisons of ground classified points and the Bare Earth DEM to ground control survey data.	TerraScan v.19 TerraModeler v.19
Convert data to orthometric elevations by applying a geoid correction for DEM creation. Generate bare earth models as triangulated surfaces. Export all surface models in ERDAS Imagine (.img) format at a 1-meter pixel resolution.	TerraScan v.19 ArcMap v. 10.3.1 LasProjector v.1.2 (NV5 GEOSPATIAL) LPD v 3.0.28 (NV5 GEOSPATIAL)
Export intensity images layered under DZ Orthos as GeoTIFFs at a 1-meter pixel resolution.	ArcMap v.10.3.1 Las Product Creator v.3.4 (NV5 GEOSPATIAL)
Export standard deviation of ground, bathymetric bottom, and submerged objects in ERDAS Imagine (.img) format at a 1-meter pixel resolution	LAS Tools

Topobathymetric DEMs

Creating digital elevation models (DEMs) presents a challenge with respect to interpolation of areas with no returns. Traditional DEMs are “unclipped”, meaning areas lacking ground returns are interpolated from neighboring ground returns, with the assumption that the interpolation is close to reality. In bathymetric modeling, these assumptions are prone to error because a lack of bathymetric returns can indicate a change in elevation that the laser can no longer map due to increased depths. The resulting void areas may suggest greater depths, rather than similar elevations from neighboring bathymetric bottom returns. Therefore, NV5 Geospatial created a polygon of bathymetric voids to delineate areas outside of successfully mapped bathymetry. This shapefile was used to control the extent of the delivered clipped topobathymetric model and to avoid false triangulation across areas in the water with no returns. Insufficiently mapped areas were identified by triangulating bathymetric bottom points with an edge length maximum of 4.56 meters. This ensured all areas of no returns larger than 9 m^2 were identified as bathymetric data voids.

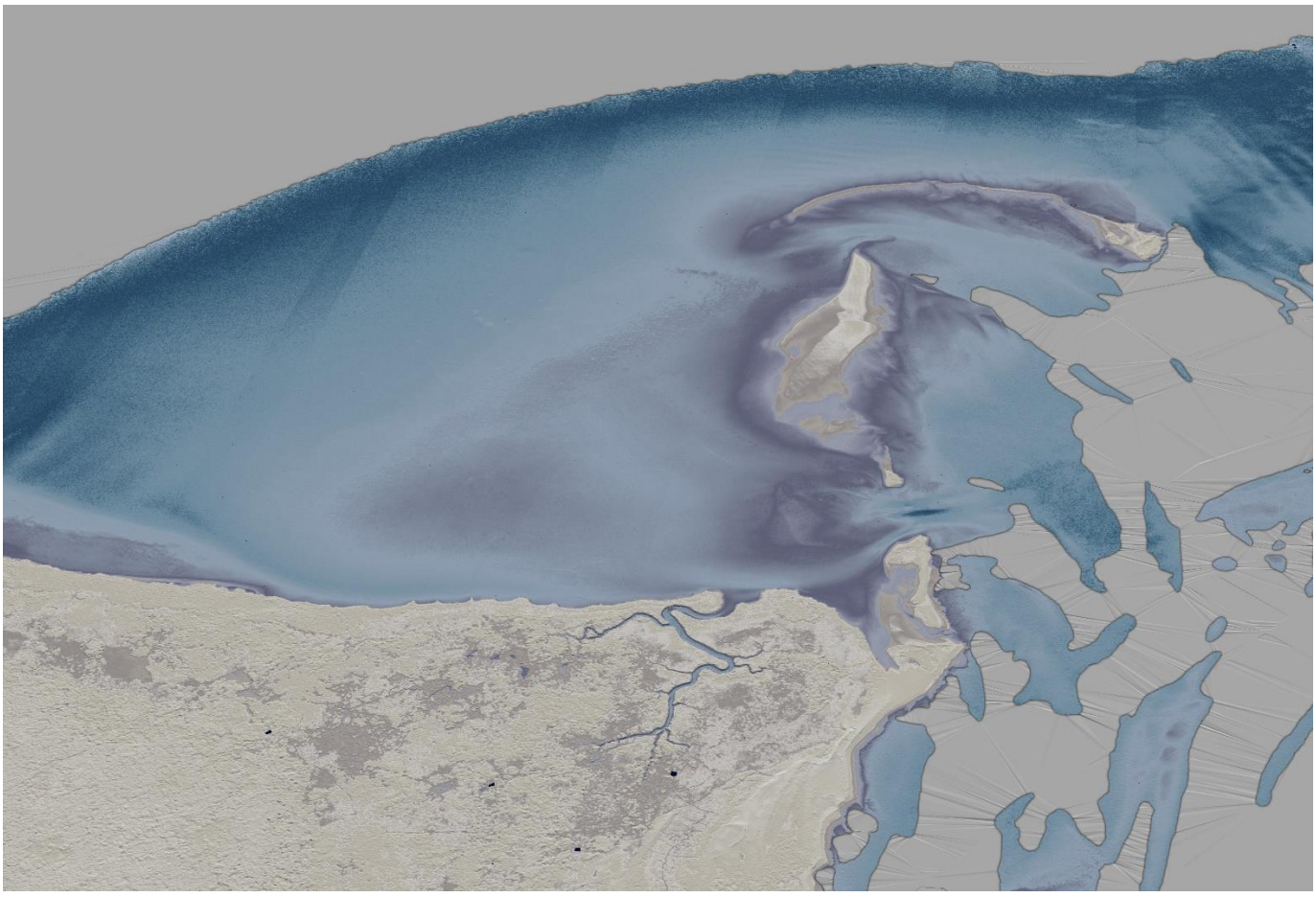

Figure 14: View of Parched Corn Bay, the gridded bare earth model is colored by elevation

LiDAR Point Density

The acquisition parameters were designed to acquire an average first-return density of 4 points/m^2. First return density describes the density of pulses emitted from the laser that return at least one echo to the system. Multiple returns from a single pulse were not considered in first return density analysis. Some types of surfaces (e.g., breaks in terrain, water and steep slopes) may have returned fewer pulses than originally emitted by the laser.

The density of ground and bathymetric bottom classified returns was also analyzed for this project. Terrain character, land cover, and ground surface reflectivity all influenced the density of ground surface returns. In vegetated areas, fewer pulses may have penetrated the canopy, resulting in lower ground density. Similarly, the density of bathymetric bottom returns was influenced by turbidity, depth, and bottom surface reflectivity. In turbid areas, fewer pulses may have penetrated the water surface, resulting in lower bathymetric density.

Detailed density statistics were provided with each lidar delivery and may be referenced in the corresponding lidar QC reports; however, average first-return density of the NOAA Hurricane Florence topobathymetric Lidar project was found to routinely exceed 10 points/m^2, while ground and bathymetric bottom classified density was routinely greater than 2 points/m^2.

LiDAR Accuracy Assessments

The accuracy of the LiDAR data collection can be described in terms of absolute accuracy (the consistency of the data with external data sources) and relative accuracy (the consistency of the dataset with itself). See Appendix A for further information on sources of error and operational measures used to improve relative accuracy.

Lidar Non-Vegetated Vertical Accuracy (NVA)

Absolute accuracy was assessed using Non-vegetated Vertical Accuracy (NVA) reporting designed to meet guidelines presented in the FGDC National Standard for Spatial Data Accuracy[7]. NVA compares known ground check point data that were withheld from the calibration and post-processing of the Lidar point cloud to the triangulated surface generated by the classified Lidar point cloud, as well as to the derived gridded bare earth DEM. NVA is a measure of the accuracy of Lidar point data in open areas where the Lidar system has a high probability of measuring the ground surface and is evaluated at the 95% confidence interval (1.96 * RMSE).

[7] Federal Geographic Data Committee, ASPRS POSITIONAL ACCURACY STANDARDS FOR DIGITAL GEOSPATIAL DATA EDITION 1, Version 1.0, NOVEMBER 2014. https://www.asprs.org/a/society/committees/standards/Positional_Accuracy_Standards.pdf.

The mean and standard deviation (sigma σ) of divergence of the ground surface model from ground check point coordinates are also considered during accuracy assessment. These statistics assume the error for x, y and z is normally distributed, and therefore the skew and kurtosis of distributions are also considered when evaluating error statistics.

NC-1901-TB-C

For the NC-1901-TB-C lidar project area, 51 ground check points were withheld from the calibration and post-processing of the lidar point cloud, with resulting non-vegetated vertical accuracy of 0.061 meters as compared to the classified LAS, and 0.055 meters against the bare earth DEM, with 95% confidence (Table 11). The spatial distribution of these results is shown in Figure 15 and Figure 16. Absolute accuracy for this area was also assessed against 2,994 ground control points (Figure 17).

Table 11: NC-1901-TB-C Absolute accuracy results

NC-1901-TB-C Absolute Vertical Accuracy			
	NVA, as compared to Classified LAS	**NVA, as compared to Bare Earth DEM**	**Ground Control Points***
Sample	51 points	51 points	2,994 points
95% Confidence (1.96*RMSE)	0.061 m	0.054 m	0.054 m
Average	0.000 m	-0.001 m	-0.003 m
Median	-0.003 m	0.001 m	-0.003 m
RMSE	0.031 m	0.027 m	0.027 m
Standard Deviation (1σ)	0.032 m	0.028 m	0.027 m

**These points were utilized in calibration and post-processing*

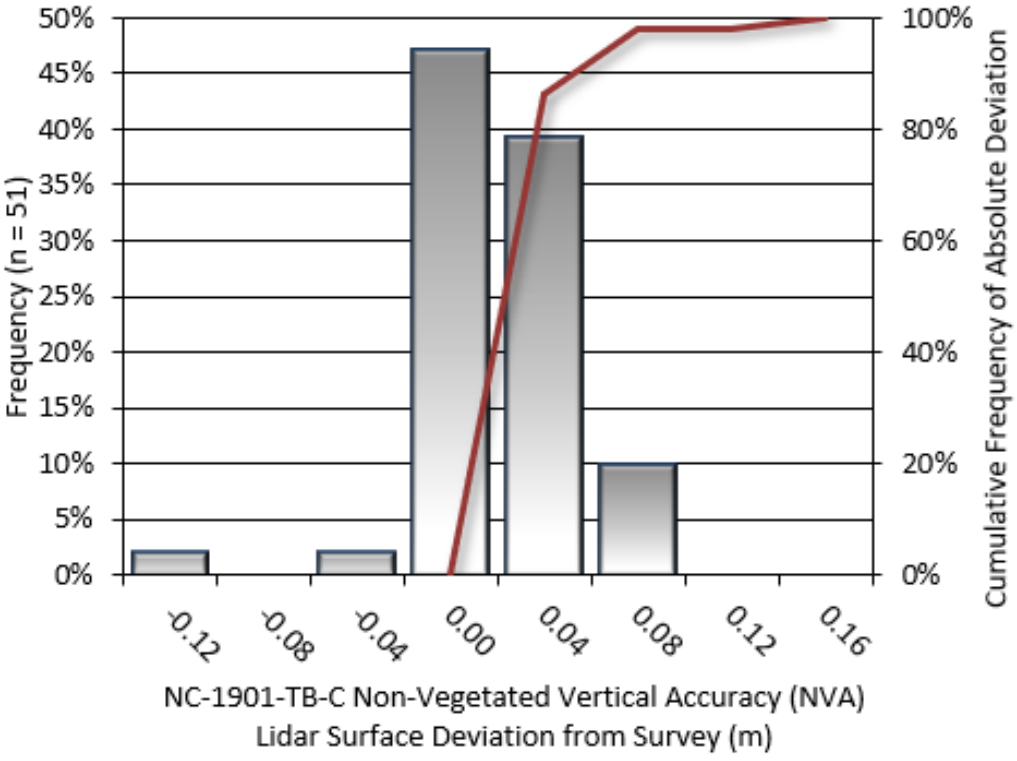

Figure 15: NC-1901-TB-C, Frequency histogram for classified LAS deviation from ground check point values

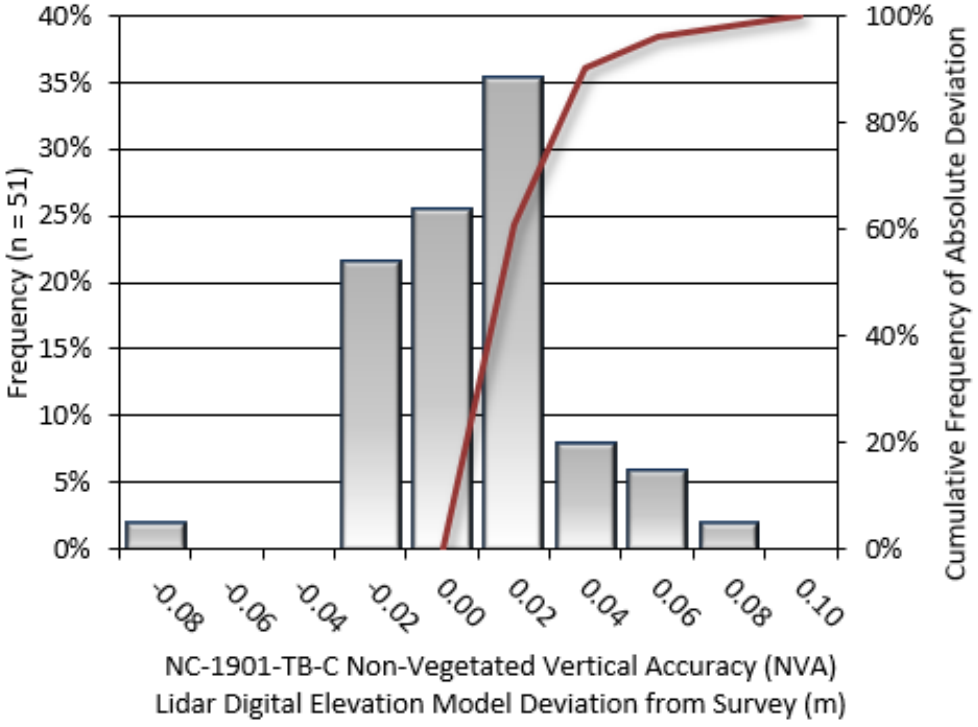

Figure 16: NC-1901-TB-C, Frequency histogram for Lidar bare earth DEM deviation from ground check point values

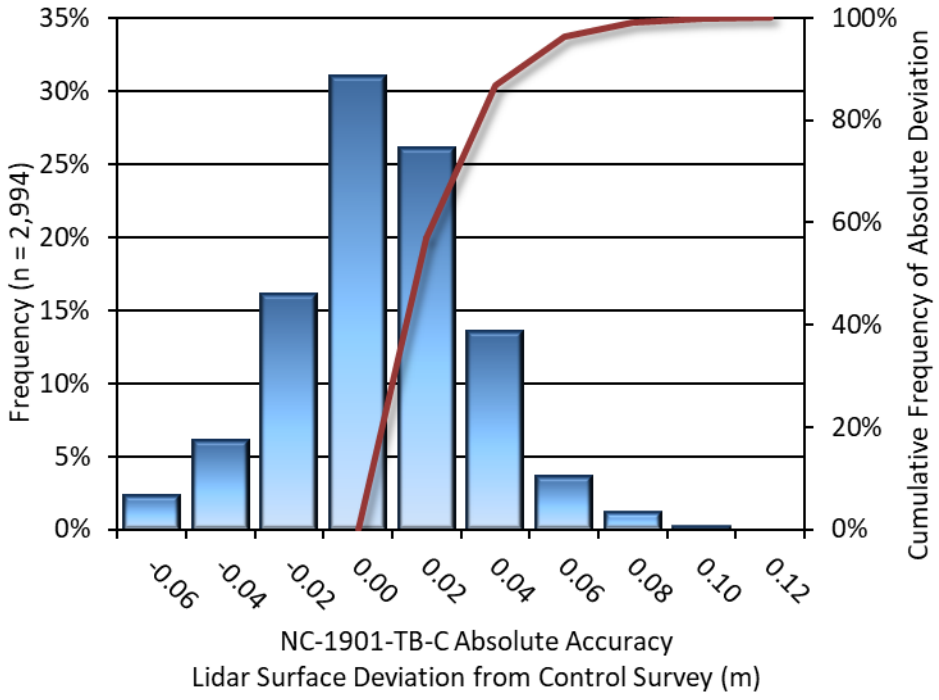

Figure 17: NC-1901-TB-C, Frequency histogram for Lidar surface deviation ground control point values

NC-1902-TB-C

For the NC-1902-TB-C lidar project area, 54 ground check points were withheld from the calibration and post-processing of the lidar point cloud, with resulting non-vegetated vertical accuracy of 0.078 meters as compared to the classified LAS, and 0.068 meters against the bare earth DEM, with 95% confidence (Table 12). The spatial distribution of these results is shown in Figure 18 and Figure 19. Absolute accuracy for this area was also assessed against 2,851 ground control points (Figure 20).

Table 12: NC-1902-TB-C Absolute accuracy results

NC-1902-TB-C Absolute Vertical Accuracy			
	NVA, as compared to Classified LAS	**NVA, as compared to Bare Earth DEM**	**Ground Control Points***
Sample	54 points	54 points	2,851 points
95% Confidence (1.96*RMSE)	0.078 m	0.068 m	0.059 m
Average	0.008 m	-0.002 m	0.000 m
Median	0.006 m	-0.004 m	0.000 m
RMSE	0.040 m	0.035 m	0.030 m
Standard Deviation (1σ)	0.039 m	0.035 m	0.030 m

**These points were utilized in lidar calibration and post-processing*

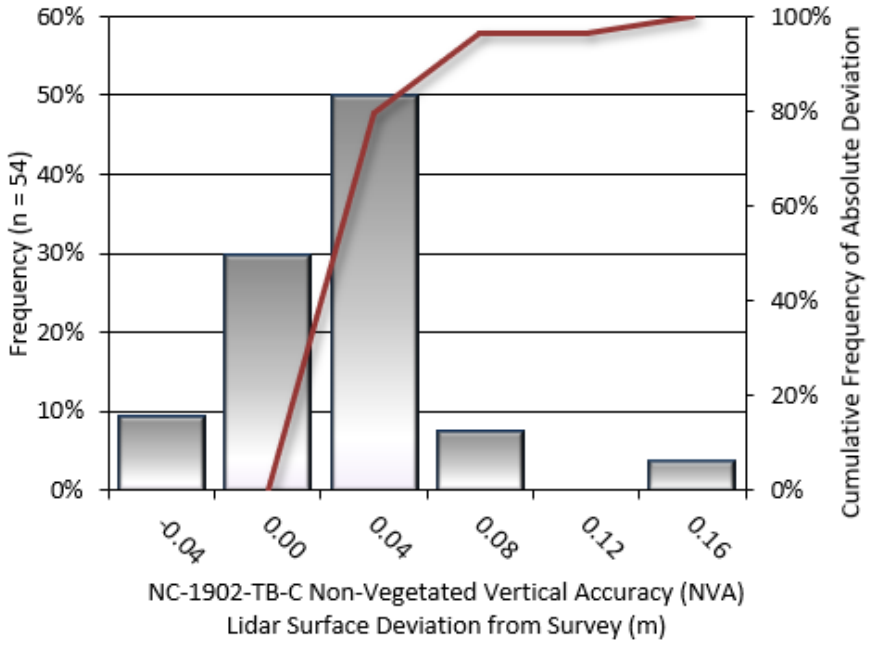

Figure 18: NC-1902-TB-C, Frequency histogram for classified LAS deviation from ground check point values

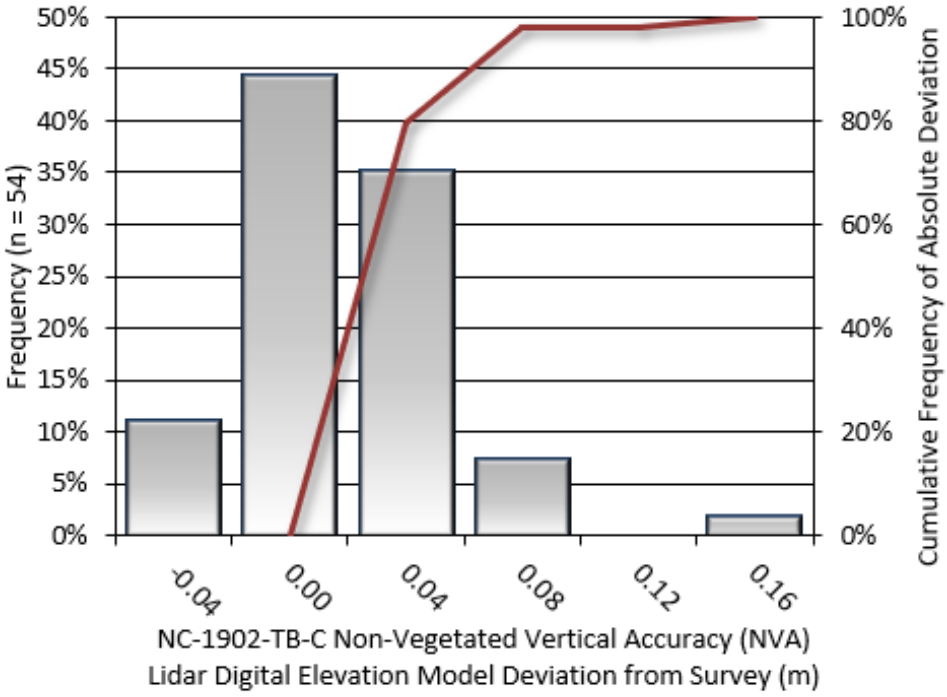

Figure 19: NC-1902-TB-C, Frequency histogram for Lidar bare earth DEM deviation from ground check point values

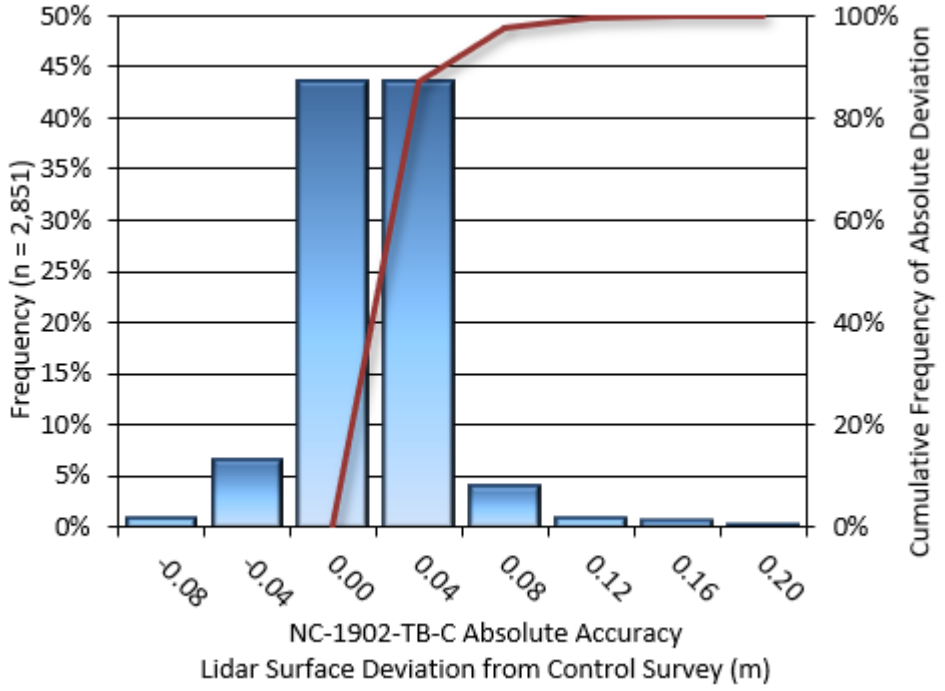

Figure 20: NC-1902-TB-C, Frequency histogram for Lidar surface deviation ground control point values

NC-1903-TB-C

For the NC-1903-TB-C lidar project area, 81 ground check points were withheld from the calibration and post-processing of the lidar point cloud, with resulting non-vegetated vertical accuracy of 0.067 meters as compared to the classified LAS, and 0.062 meters against the bare earth DEM, with 95% confidence (Table 13). The spatial distribution of these results is shown in Figure 21 and Figure 22. Absolute accuracy for this area was also assessed against 4,862 ground control points (Figure 23).

Table 13: NC-1903-TB-C Absolute accuracy results

NC-1903-TB-C Absolute Vertical Accuracy			
	NVA, as compared to Classified LAS	**NVA, as compared to Bare Earth DEM**	**Ground Control Points***
Sample	81 points	81 points	4,862 points
95% Confidence (1.96*RMSE)	0.067 m	0.062 m	0.054 m
Average	0.012 m	0.005 m	0.002 m
Median	0.013 m	0.002 m	0.003 m
RMSE	0.034 m	0.032 m	0.027 m
Standard Deviation (1σ)	0.032 m	0.032 m	0.027 m

**These points were utilized in calibration and post-processing*

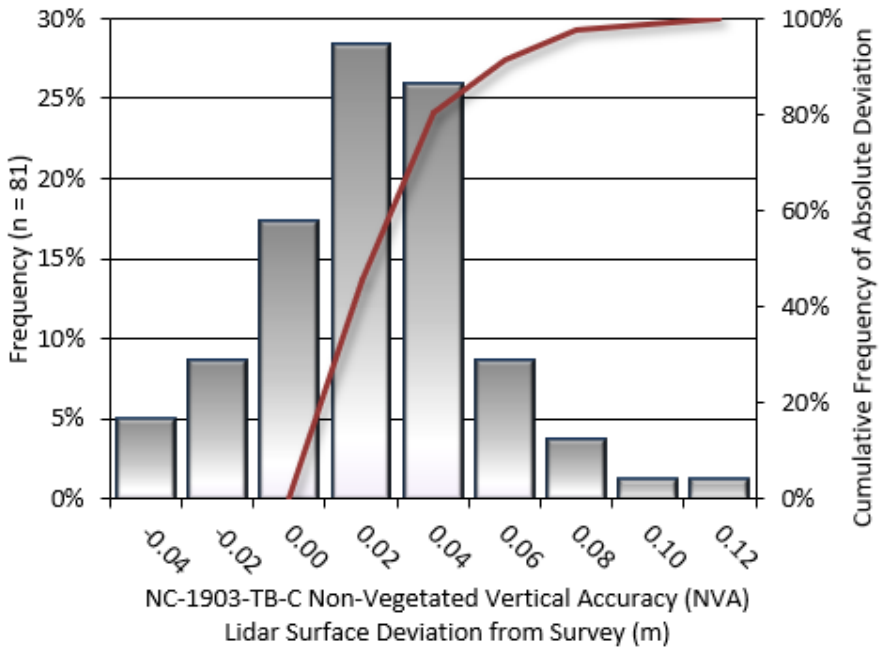

Figure 21: NC-1903-TB-C, Frequency histogram for classified LAS deviation from ground check point values

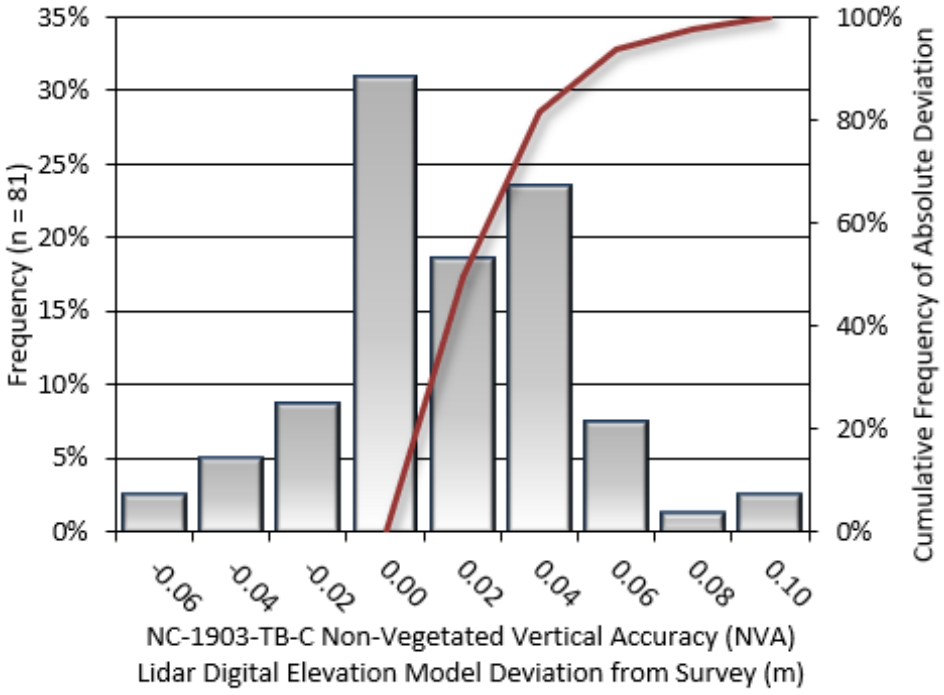

Figure 22: NC-1903-TB-C, Frequency histogram for Lidar bare earth DEM deviation from ground check point values

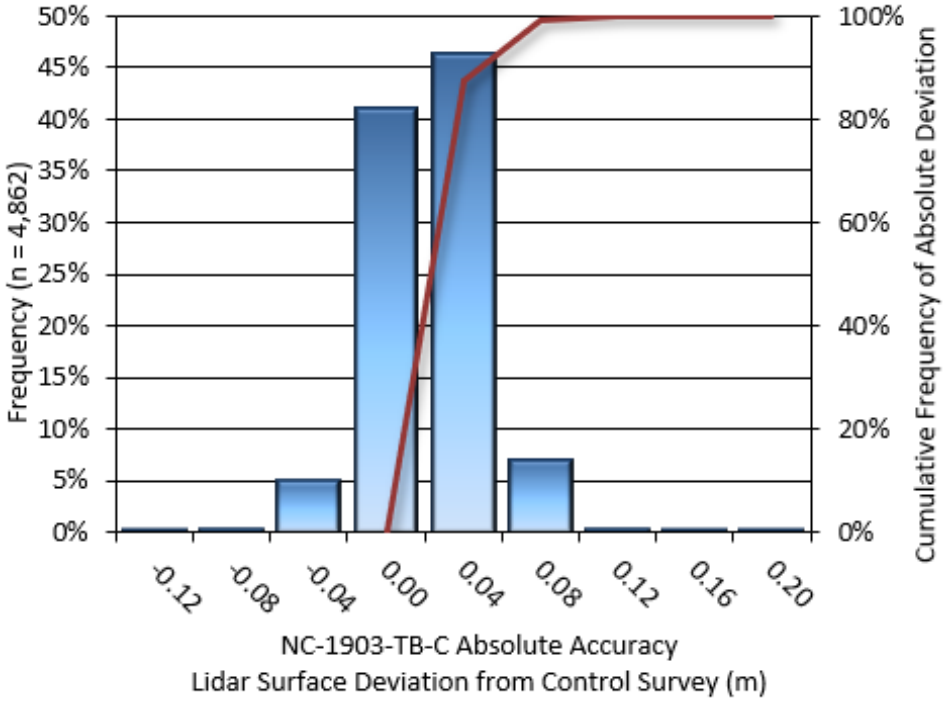

Figure 23: NC-1903-TB-C, Frequency histogram for Lidar surface deviation ground control point values

Lidar Bathymetric Vertical Accuracies

Bathymetric vertical accuracy is evaluated using submerged check point data compared to the bathymetric classified Lidar points. BVA is evaluated at the 95% confidence interval. Results by sub-area are presented in Table 14 below, and in Figure 24 through Figure 26.

Table 14: Bathymetric Vertical Accuracy for the NOAA Hurricane Florence Topobathymetric Lidar Project

Bathymetric Vertical Accuracy (BVA)			
	NC-1901-TB-C	**NC-1902-TB-C**	**NC-1903-TB-C**
Sample	218 points	482 points	258 points
95% Confidence (1.96*RMSE)	0.105 m	0.146 m	0.091 m
Average Dz	0.010 m	0.017 m	0.006 m
Median	0.009 m	0.016 m	0.010 m
RMSE	0.053 m	0.075 m	0.047 m
Standard Deviation (1σ)	0.053 m	0.073 m	0.046 m

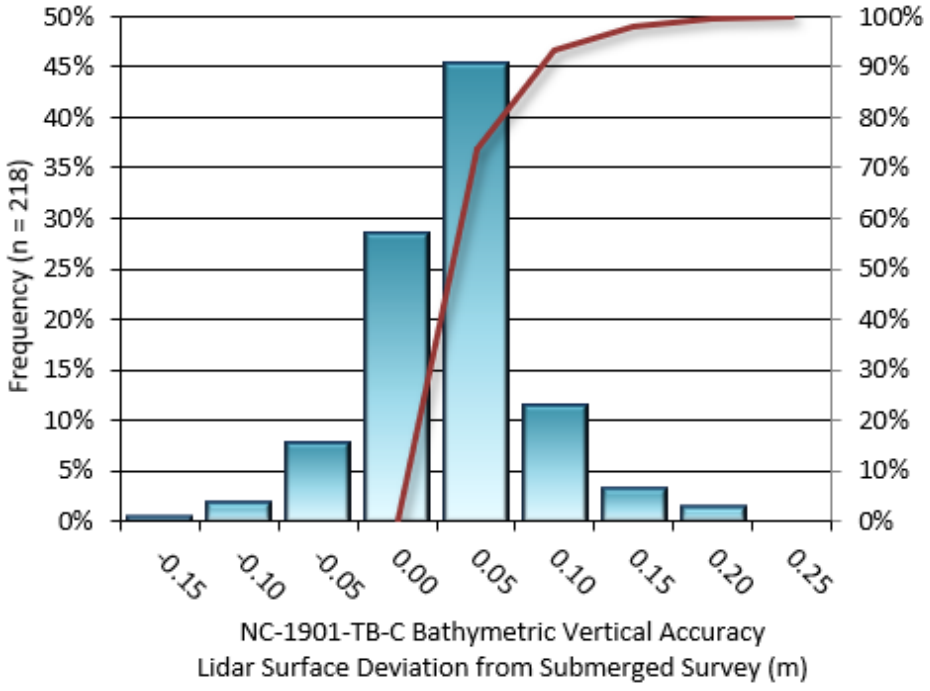

Figure 24: NC-1901-TB-C, Frequency histogram for Lidar surface deviation from submerged check point values

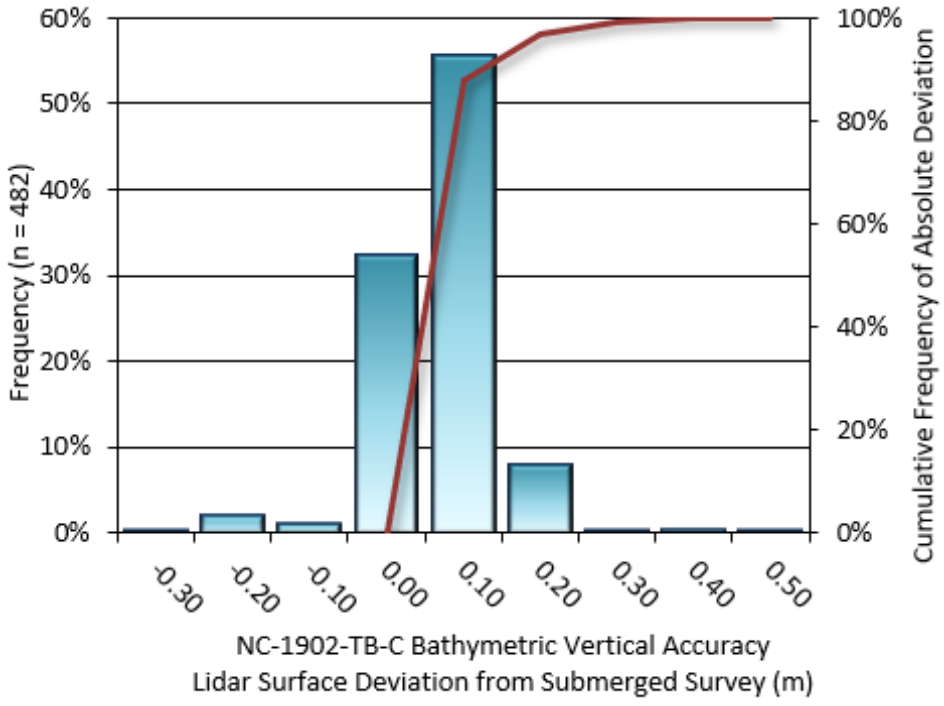

Figure 25: NC-1902-TB-C, frequency histogram for Lidar surface deviation from submerged check point values

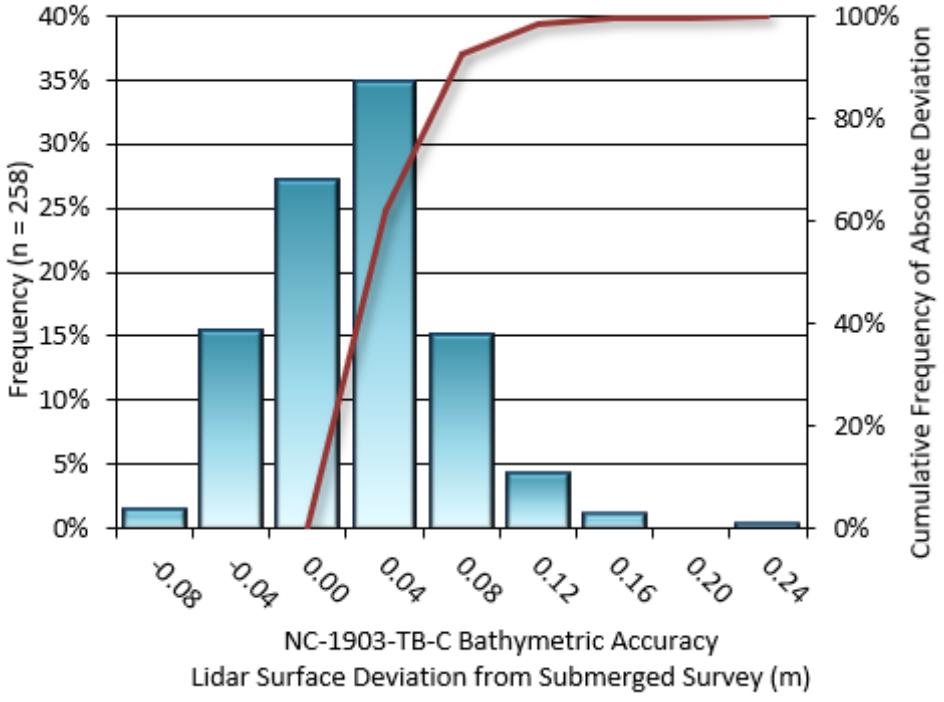

Figure 26: NC-1903-TB-C, frequency histogram for Lidar surface deviation from submerged check point values

Lidar Vegetated Vertical Accuracies

Vegetated Vertical Accuracy (VVA) compares known ground check point data collected over vegetated surfaces using land class descriptions to the triangulated ground surface generated by the ground classified Lidar points. VVA is evaluated at the 95th percentile (Table 15). The spatial distribution of each sub-area is displayed in Figure 27 through Figure 29.

Table 15: Vegetated Vertical Accuracy for the NOAA Hurricane Florence Topobathymetric Lidar Project

Vegetated Vertical Accuracy, (as compared to Bare Earth DEM) (VVA)			
	NC-1901-TB-C	**NC-1902-TB-C**	**NC-1903-TB-C**
Sample	46 points	17 points	57 points
Average Dz	0.058 m	0.072 m	0.072 m
Median	0.037 m	0.058 m	0.066 m
RMSE	0.079 m	0.119 m	0.103 m
Standard Deviation (1σ)	0.055 m	0.098 m	0.075 m
95th Percentile	0.161 m	0.234 m	0.188 m

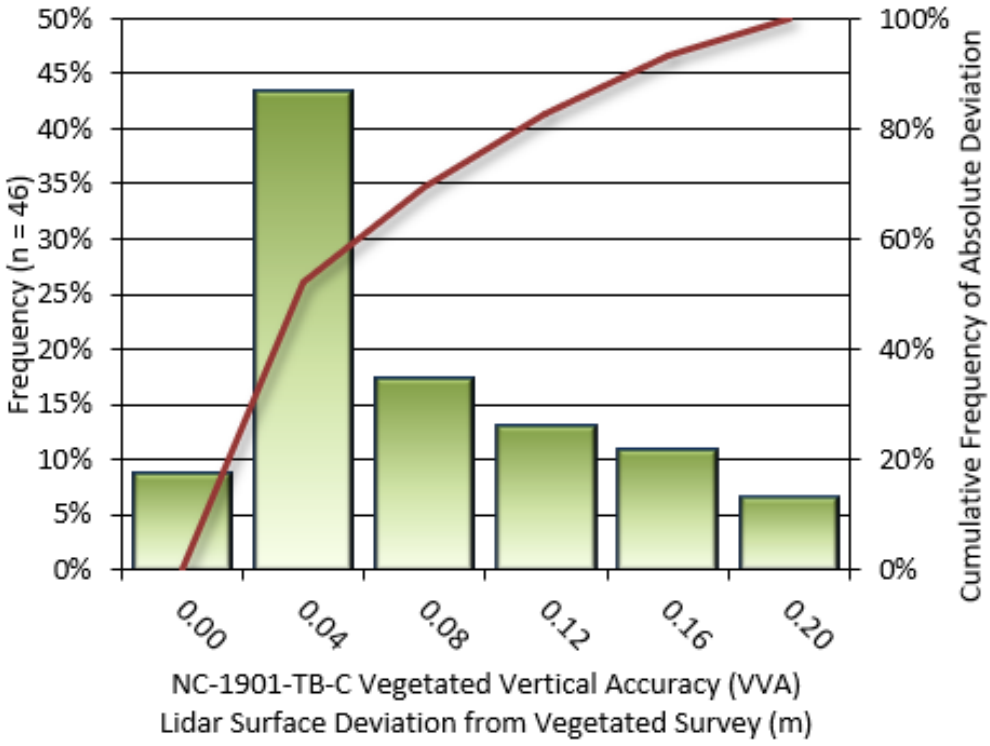

Figure 27: NC-1901-TB-C, Frequency histogram for lidar surface model deviation from vegetated check point values

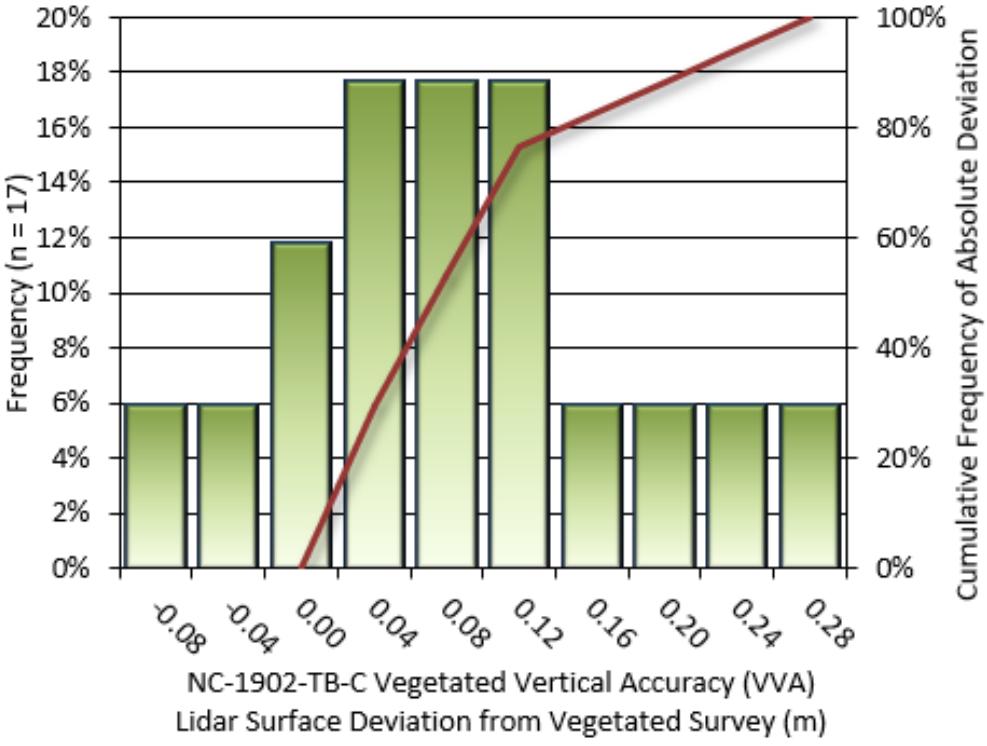

Figure 28: NC-1902-TB-C, Frequency histogram for lidar surface model deviation from vegetated check point values

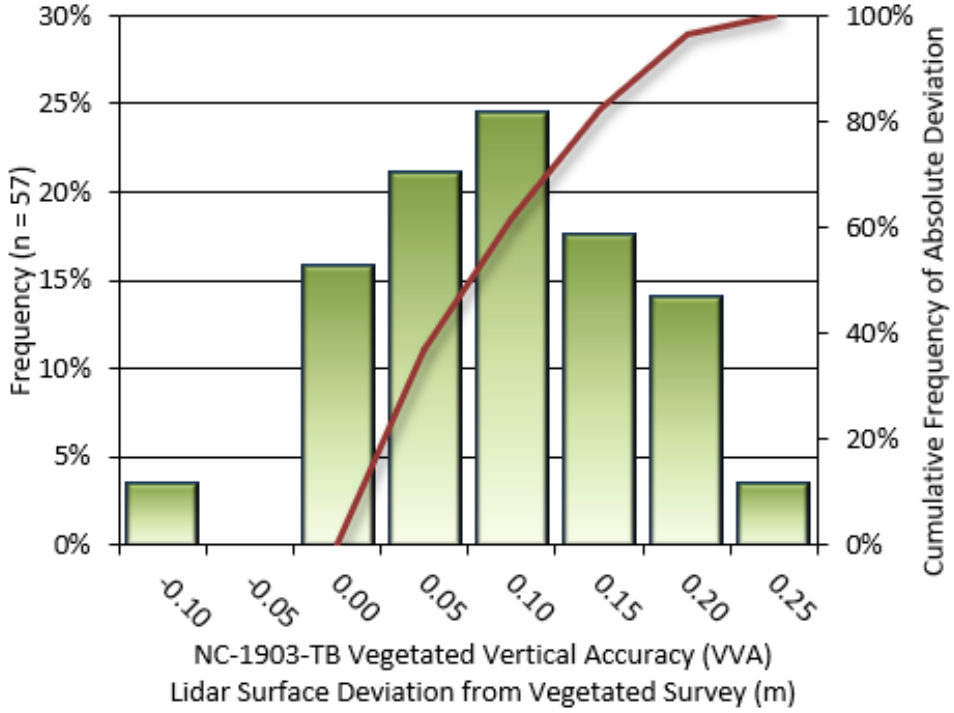

Figure 29: **NC-1903-TB-C, Frequency histogram for lidar surface model deviation from vegetated check point values**

Lidar Relative Vertical Accuracy

Relative vertical accuracy refers to the internal consistency of the data set as a whole: the ability to place an object in the same location given multiple flight lines, GPS conditions, and aircraft attitudes. When the Lidar system is well calibrated, the swath-to-swath vertical divergence is low (<0.10 meters). The relative vertical accuracy was computed by comparing the ground surface model of each individual flight line with its neighbors in overlapping regions. Comparison of 7,789 flightline surfaces resulted in an RMSEDz line to line relative vertical accuracy of 0.039 meter for the NOAA Hurricane Florence Lidar project (Table 16). The frequency plot for relative vertical accuracy deviations is shown in Figure 30.

Table 16: Relative accuracy results

Relative Accuracy	
Sample	7,789 surfaces
Average	0.024 m
Median	0.026 m
RMSE	0.039 m
Standard Deviation (1σ)	0.021 m
1.96σ	0.042 m

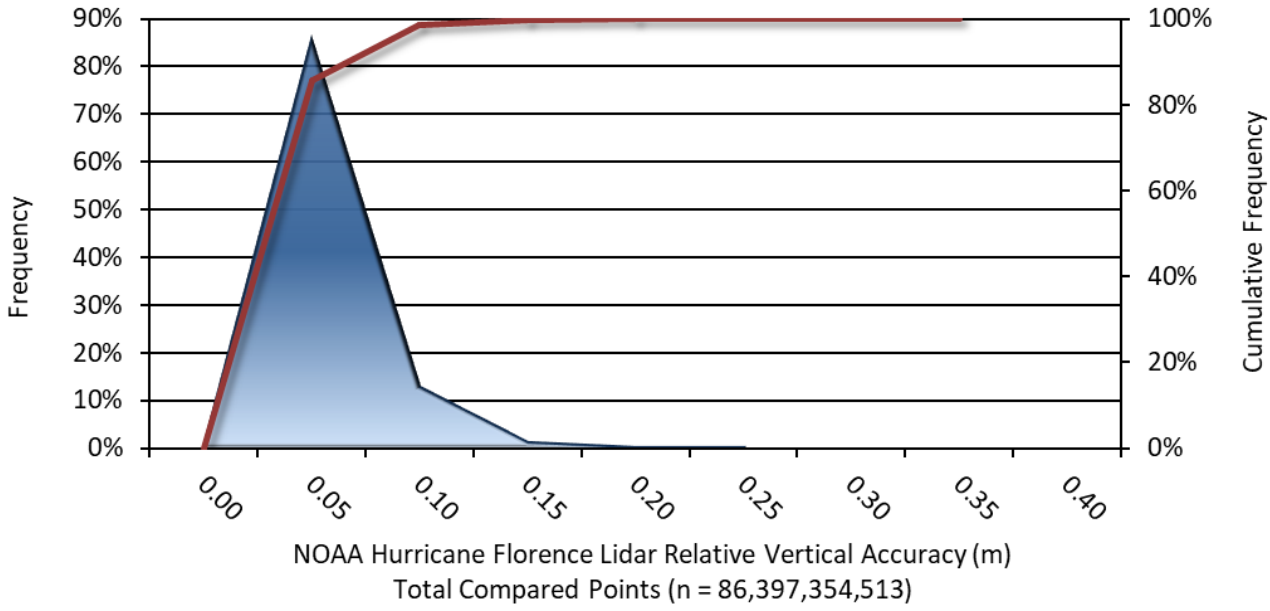

Figure 30: Frequency plot for relative vertical accuracy between flight lines

Lidar Horizontal Accuracy

LiDAR horizontal accuracy is a function of Global Navigation Satellite System (GNSS) derived positional error, flying altitude, and INS derived attitude error. The obtained $RMSE_r$ value is multiplied by a conversion factor of 1.7308 to yield the horizontal component of the National Standards for Spatial Data Accuracy (NSSDA) reporting standard where a theoretical point will fall within the obtained radius 95 percent of the time. Based on a flying altitude of 400 meters, an IMU error of 0.006 decimal degrees, and a maximum GNSS positional error of 0.023 meters, this project was compiled to meet 0.14 m horizontal accuracy at the 95% confidence level (Table 17).

Table 17: Horizontal Accuracy

Horizontal Accuracy	
$RMSE_r$	0.078 m
ACC_r	0.14 m

Digital Imagery Accuracy Assessment

Image accuracy was measured by air target locations and independent ground survey points. NV5 Geospatial provided imagery accuracy assessment along with the imagery deliverable reporting (Table 2), as *NC1901_NC1902_NC1903_Hurricane_Florence_AT_Report_QSI.doc.*

Lessons Learned

For the lidar processing aspect of the Hurricane Florence project, the use of the Leica Chiroptera CH4X sensor presented the greatest workflow challenges and adaptations which will prove useful in future topobathymetric lidar projects between NV5 Geospatial and NOAA. The process of determining how to integrate the Riegl sensor data with the deep channel Leica returns resulted in the development of a cut-line approach between datasets to best deal with any temporal offsets between sensors. In terms of QA/QC and data review, NV5 Geospatial struggled to establish a clear workflow and guidance for the treatment of small inland water bodies, which caused a higher than anticipated number of QC calls in early deliveries.

Additionally, this was NV5G's second project which required Total Propagated Uncertainty (TPU) deliverables, and normalization for depth in the lidar point cloud. During TPU processing, NV5 Geospatial encountered versioning issues in CBLUE software and some additional troubleshooting with "No VDatum" specifications. A workflow to produce TPU deliveries for the Leica Chiroptera CH4X sensor has yet to be developed. Overall, the TPU deliverables for NOAA projects are still being established and will require further refinement between NV5 Geospatial and NOAA on future projects.

As always, NV5 Geospatial greatly values all working partnerships and opportunities to work with the NOAA team. This project has been a large undertaking, and we are grateful for the opportunity to assist NOAA in their mapping objectives.

GLOSSARY

1-sigma (σ) Absolute Deviation: Value for which the data are within one standard deviation (approximately 68th percentile) of a normally distributed data set.

1.96 * RMSE Absolute Deviation: Value for which the data are within two standard deviations (approximately 95th percentile) of a normally distributed data set, based on the FGDC standards for Non-vegetated Vertical Accuracy (FVA) reporting.

Accuracy: The statistical comparison between known (surveyed) points and laser points. Typically measured as the standard deviation (sigma σ) and root mean square error (RMSE).

> **Absolute Accuracy:** The vertical accuracy of LiDAR data is described as the mean and standard deviation (sigma σ) of divergence of LiDAR point coordinates from ground survey point coordinates. To provide a sense of the model predictive power of the dataset, the root mean square error (RMSE) for vertical accuracy is also provided. These statistics assume the error distributions for x, y and z are normally distributed, and thus we also consider the skew and kurtosis of distributions when evaluating error statistics.
>
> **Relative Accuracy:** Relative accuracy refers to the internal consistency of the data set; i.e., the ability to place a laser point in the same location over multiple flight lines, GPS conditions and aircraft attitudes. Affected by system attitude offsets, scale and GPS/IMU drift, internal consistency is measured as the divergence between points from different flight lines within an overlapping area. Divergence is most apparent when flight lines are opposing. When the LiDAR system is well calibrated, the line-to-line divergence is low (<10 cm).
>
> **Root Mean Square Error (RMSE):** A statistic used to approximate the difference between real-world points and the LiDAR points. It is calculated by squaring all the values, then taking the average of the squares and taking the square root of the average.

Data Density: A common measure of LiDAR resolution, measured as points per square meter.

Digital Elevation Model (DEM): File or database made from surveyed points, containing elevation points over a contiguous area. Digital terrain models (DTM) and digital surface models (DSM) are types of DEMs. DTMs consist solely of the bare earth surface (ground points), while DSMs include information about all surfaces, including vegetation and man-made structures.

Intensity Values: The peak power ratio of the laser return to the emitted laser, calculated as a function of surface reflectivity.

Nadir: A single point or locus of points on the surface of the earth directly below a sensor as it progresses along its flight line.

Overlap: The area shared between flight lines, typically measured in percent. 100% overlap is essential to ensure complete coverage and reduce laser shadows.

Pulse Rate (PR): The rate at which laser pulses are emitted from the sensor; typically measured in thousands of pulses per second (kHz).

Pulse Returns: For every laser pulse emitted, the number of wave forms (i.e., echoes) reflected back to the sensor. Portions of the wave form that return first are the highest element in multi-tiered surfaces such as vegetation. Portions of the wave form that return last are the lowest element in multi-tiered surfaces.

Real-Time Kinematic (RTK) Survey: A type of surveying conducted with a GPS base station deployed over a known monument with a radio connection to a GPS rover. Both the base station and rover receive differential GPS data and the baseline correction is solved between the two. This type of ground survey is accurate to 1.5 cm or less.

Post-Processed Kinematic (PPK) Survey: GPS surveying is conducted with a GPS rover collecting concurrently with a GPS base station set up over a known monument. Differential corrections and precisions for the GNSS baselines are computed and applied after the fact during processing. This type of ground survey is accurate to 1.5 cm or less.

Scan Angle: The angle from nadir to the edge of the scan, measured in degrees. Laser point accuracy typically decreases as scan angles increase.

Native LiDAR Density: The number of pulses emitted by the LiDAR system, commonly expressed as pulses per square meter.

Relative Accuracy Calibration Methodology:

Manual System Calibration: Calibration procedures for each mission require solving geometric relationships that relate measured swath-to-swath deviations to misalignments of system attitude parameters. Corrected scale, pitch, roll and heading offsets were calculated and applied to resolve misalignments. The raw divergence between lines was computed after the manual calibration was completed and reported for each survey area.

Automated Attitude Calibration: All data were tested and calibrated using TerraMatch automated sampling routines. Ground points were classified for each individual flight line and used for line-to-line testing. System misalignment offsets (pitch, roll and heading) and scale were solved for each individual mission and applied to respective mission datasets. The data from each mission were then blended when imported together to form the entire area of interest.

Automated Z Calibration: Ground points per line were used to calculate the vertical divergence between lines caused by vertical GPS drift. Automated Z calibration was the final step employed for relative accuracy calibration.

LiDAR accuracy error sources and solutions:

Type of Error	Source	Post Processing Solution
GPS (Static/Kinematic)	Long Base Lines	None
	Poor Satellite Constellation	None
	Poor Antenna Visibility	Reduce Visibility Mask
Relative Accuracy	Poor System Calibration	Recalibrate IMU and sensor offsets/settings
	Inaccurate System	None
Laser Noise	Poor Laser Timing	None
	Poor Laser Reception	None
	Poor Laser Power	None
	Irregular Laser Shape	None

Operational measures taken to improve relative accuracy:

Low Flight Altitude: Terrain following was employed to maintain a constant above ground level (AGL). Laser horizontal errors are a function of flight altitude above ground (about 1/3000th AGL flight altitude).

Focus Laser Power at narrow beam footprint: A laser return must be received by the system above a power threshold to accurately record a measurement. The strength of the laser return (i.e., intensity) is a function of laser emission power, laser footprint, flight altitude and the reflectivity of the target. While surface reflectivity cannot be controlled, laser power can be increased and low flight altitudes can be maintained.

Reduced Scan Angle: Edge-of-scan data can become inaccurate. The scan angle was reduced to a maximum of ±20^{o} from nadir, creating a narrow swath width and greatly reducing laser shadows from trees and buildings.

Quality GPS: Flights took place during optimal GPS conditions (e.g., 6 or more satellites and PDOP [Position Dilution of Precision] less than 3.0). Before each flight, the PDOP was determined for the survey day. During all flight times, a dual frequency DGPS base station recording at 1 second epochs was utilized and a maximum baseline length between the aircraft and the control points was less than 13 nm at all times.

Ground Survey: Ground survey point accuracy (<1.5 cm RMSE) occurs during optimal PDOP ranges and targets a minimal baseline distance of 4 miles between GPS rover and base. Robust statistics are, in part, a function of sample size (n) and distribution. Ground survey points are distributed to the extent possible throughout multiple flight lines and across the survey area.

50% Side-Lap (100% Overlap): Overlapping areas are optimized for relative accuracy testing. Laser shadowing is minimized to help increase target acquisition from multiple scan angles. Ideally, with a 50% side-lap, the nadir portion of one flight line coincides with the swath edge portion of overlapping flight lines. A minimum of 50% side-lap with terrain-followed acquisition prevents data gaps.

Opposing Flight Lines: All overlapping flight lines have opposing directions. Pitch, roll and heading errors are amplified by a factor of two relative to the adjacent flight line(s), making misalignments easier to detect and resolve.

APPENDIX B - AT REPORT

Aerotriangulation Report
Hurricane Florence – NC1901, NC1902 and NC1903
June 2020

Area Covered

The project area covers two (3) adjacent Areas of Interest (AOIs) aligned north to south along the eastern shoreline of the North Carolina. The AOIs extend from just north of shorelines of Albemarle and Pamlico Sounds south to Winyah Bay in Georgetown County, South Carolina.

Florence – Area 01

The project area, referenced as NC1901 and "Cape Hatteras to Winyah Bay, NC," covers one Area of Interest (AOI) along the eastern shoreline of South Carolina (northern 1/3) and North Carolina (southern 2/3).

The AOI extends from just south of Winyah Bay in Georgetown County, South Carolina and runs northwest to Cape Hatteras in Dare County, North Carolina.

The AOI covers approximately 1,528 square miles and 3,024 linear miles of shoreline.

NC1901 extends roughly 240 kilometers north-south, 360 kilometers east-west, and sweeps southwest-to-northeast in a narrow band hugging the coastline along 3 large bays in northeast South Carolina and southeast North Carolina.

The AOI stretches from Winyah Bay in the south, northeast along Long Bay to Cape Fear (crossing the state line), and then further northeast along Onslow Bay to Cape Lookout, and then again further northeast along Raleigh Bay to Cape Hatteras.

NC1901 can be geographically described as three adjoining sections running southwest to northeast along the coast.

The first includes all of the shoreline from just south of Winyah Bay northeastward to Cape Fear, encompassing the entire shoreline of Long Bay, and including Myrtle Beach and its neighboring communities. The AOI crosses the State line just north of North Myrtle Beach near the Little River Inlet. On the ocean side, the AOI extends out from the shore roughly 300-500 meters on average, extending further into the ocean, as needed, to include jetties and significant underwater features of concern (primarily sediment deposits at the mouths of outlets to the sea or surrounding the Capes themselves). This section of the AOI includes the shoreline portions of Georgetown and Horry Counties in South Carolina, and Brunswick County in southeastern North Carolina.

Moving northeast, the second section of the AOI includes all of the shoreline from Cape Fear to Cape Lookout, encompassing the entire shoreline of Onslow Bay, and including Carolina Beach, Wrightsville Beach, portions of Camp Lejeune, Swansboro, Morehead City and Beaufort. On the ocean side, the AOI extends out from the shore roughly 300-500 meters on average, extending further into the ocean, as

needed, to include jetties and significant underwater features of concern (primarily sediment deposits at the mouths of outlets to the sea or surrounding the Capes themselves). Inland, the AOI includes a short extension up the Cape Fear River to include portions of Wilmington, NC. Further northeast, the AOI includes two additional inland extensions to encompass the New River estuary (including Stump Sound, Morgan Bay, and shore-facing portions of Jacksonville, NC). This section's northeastern end encompasses Bogue Sound, Back Sound, and the barrier islands extending out to Cape Lookout; this section of the AOI also includes Morehead City, the Newport River estuary (plus a short extension northward along the Intracoastal Waterway), and the North River estuary. This section of the AOI includes the shoreline portions of New Hanover, Pender, Onslow, and Carteret Counties in eastern North Carolina.

Moving further northeast, the third section of the AOI includes all of the shoreline from Cape Lookout to Cape Hatteras, encompassing the entire shoreline of Raleigh Bay and the barrier islands extending from Cape Lookout to Cape Hatteras (Core Banks, Portsmouth, Ocracoke, and Hatteras). This also includes the Ocracoke and Hatteras Inlets to Pamlico Sound, and the small towns of Portsmouth, Ocracoke, and Hatteras, NC). On the ocean side, the AOI extends out from the shore roughly 300-500 meters on average, extending further into the ocean, as needed, to include jetties and significant underwater features of concern (primarily sediment deposits at the mouths of outlets to the sea or surrounding the Capes themselves). Inland, the AOI encompasses Core Sound, and Sound-facing portions of Carteret County, including Jarret, Nelson, and Thorofare Bays. The AOI extends northward into Pamlico sound to encompass all of Cedar island, and then narrows back down moving northward (towards Portsmouth Island) until it approaches Ocracoke Inlet, where it again extends back into a portion of Pamlico Sound (and shipping lanes) as much as 16 kilometers. Further northeast, the AOI narrows to encompass Ocracoke Island, extending back into Pamlico Sound 3-5 kilometers. At its northeastern end, the AOI again widens to encompass the Hatteras Inlet to Pamlico Sound and the portion of Hatteras Island from the inlet to just north of Buxton, NC. On the Sound side, the AOI extends 6-9 kilometers back into Pamlico Sound along the southern portions of Hatteras Island to encompass the Bird Islands and surrounding shallow waters. This section of the AOI includes the shoreline portions of Carteret, Hyde, and Dare Counties in northeastern North Carolina.

The project is located approximately between 33°10'41" and 35°19'34" North Latitude, and 75°31'00" and 79°21'00" West Longitude.

For the context of this specific Project Area report, it is important to understand that the NC1901 Project Area has two sibling Project Areas (NC1902 & NC1903) immediately contiguous to its north (at Cape Hatteras), as well as to its northwest (by Cedar Island on the south side of Pamlico Sound).

Florence – Area 02

The project area, referenced as NC1902 and "*Cape Henry, VA to Cape Hatteras, NC,*" covers a single Area of Interest (AOI) along the eastern shoreline of North Carolina (north of Cape Hatteras to the Virginia state line) and Virginia (from the NC state line to Cape Henry, VA (i.e., the south edge of the wide opening to Chesapeake Bay).

The AOI extends from just north of Cape Hatteras in Dare County, North Carolina north-northeastward to Rodanthe, NC on the outer banks, then angles northwestward to encompass Kill Devil Hills, the barrier island running to and beyond the NC/VA state line, and up to Cape Henry in Virginia City, VA.

The AOI covers an area of approximately 701 square miles and 1,060 linear miles of shoreline.

NC1902 extends roughly 188 kilometers north-south, and 58 kilometers east-west, and is aligned primarily south-southeast to north-northwest. The southern 37 kilometers of the AOI runs slightly northeast from Cape Hatteras, but turns north-northwestward for the remainder of its course, running north to the south lip of the Chesapeake at Cape Henry.

The AOI begins just north of Cape Hatteras (adjoining NC1901), and includes all of the shoreline from there northeastward to Rodanthe, NC. The AOI then turns north-northwest, encompassing the Pea Island NWR, Oregon Inlet, and Bodie Island, including Nags Head, Kill Devil Hills, and Kitty Hawk. The AOI continues to run NNW along the barrier island that runs up to & beyond the NC/VA state line. In Virginia, the barrier island rejoins the mainland north of Back Bay, and continues NNW within the City of Virginia Beach to Cape Henry.

On the ocean side, the AOI extends out from the shore roughly 400-500 meters on average, extending further into the ocean at Oregon Inlet to include underwater features of concern (e.g., sediment deposits seaward of the inlet opening).

“Landward” at its south end, the AOI extends back from Hatteras Island close to 10 kilometers into Pamlico Sound, but this steadily narrows as it moves north to just 2 kilometers back into the Sound at Rodanthe, NC; the AOI does flare out to encompass all of Gull Island and its surrounding waters. Northward of Rodanthe, the inland side of the AOI again widens westward into the north end of Pamlico Sound, extending roughly 10 kilometers to the west of Oregon Inlet (covering the Davis Channel and other features important to navigation and safety). North of Oregon Inlet, the AOI again narrows to extend just 5 kilometers into the far north end of Pamlico Sound. The AOI again flares out to the northwest and into Croatan Sound as it encompasses Roanoke Island, Roanoke Sound, and two distinct extensions to the west covering the areas surrounding the US 64/264 bridges to Roanoke Island. The AOI bends sharply around the north and northeast sides of Roanoke Island remaining close to the island’s shore; the AOI then makes two sharp right angle turns just north of the bridge between Roanoke Island and Bodie Island (barrier island), and heads back north along the Albemarle Sound side of Nags Head, Kill Devil Hills, and Kitty Hawk; again, remaining just a couple hundred meters offshore in the Sound. West of Kitty Hawk, the AOI shifts slightly westward across the opening between Currituck Sound and Albemarle Sound, makes landfall at Powells Point and runs northwestward down the center of the Powells Point peninsula until it flares out again to the west to encompass all of the Currituck Sound-facing shore areas on the mainland, including Mackay and Knotts Islands and the North Landing River’s estuary (and crossing the NC/VA state line). The AOI then narrows back towards the shoreline just west of Back Bay (but encompassing all of its Bay-facing shoreline area), and heads NNW through the City of Virginia Beach and Cape Henry. This most northern portion of the AOI forms a wedge roughly 10 kilometers wide at the north end of Back Bay narrowing northward to just over 5 kilometers by Cape Henry.

The AOI includes shoreline portions of Dare and Currituck Counties in North Carolina, and the City of Virginia Beach in Virginia.

The project is located approximately between 35°15'36"and 36°56'04" North Latitude, and 75°27'20" and 76°06'04" West Longitude.

For the context of this specific Project Area report, it is important to understand that the NC1902 Project Area has two sibling Project Areas (NC1901 & NC1903) immediately contiguous and to its south (at Cape Hatteras) and to its west (along Albemarle and Pamlico Sound).

Florence – Area 03

The project area, referenced as NC1903 and "*Albemarle Sound to Neuse River, NC*" covers a large, single Area of Interest (AOI) along the (mostly) eastern shorelines of Pamlico and Albemarle Sounds in North Carolina.

The AOI covers an area of approximately 2,453 square miles and 2,427 linear miles of shoreline.

NC1903 extends roughly 172 kilometers north-south, and 130 kilometers east-west, and is serpentine in shape, roughly hugging the shorelines of Albemarle and Pamlico Sounds and their primary tributaries / estuaries and two broad "peninsulas" between those tributaries. The AOI specifically excludes portions of these peninsulas well inland of the Sounds. The AOI includes a narrow corridor that cuts across the large northern peninsula just north of Lake Mattamuskeet covering the Alligator River - Pungo River Canal, part of the Intracoastal Waterway).

At its northeast end, the AOI abuts NC1902 in Currituck County just to the northwest of Kitty Hawk and the Wright Memorial Bridge. It then zig-zags westward, remaining inland of Albemarle Sound and it various tributary / estuaries, including the following rivers: North, Pasquotank, Little, and Perquimans. The AOI also encompasses Elizabeth City and Edenton. The AOI crosses the Chowan River just north of the US 17 Bridge across the river's entrance into Albemarle Sound. West of the Chowan River, the AOI turns south, encompassing just a small portion of the Roanoke River to the west of where it enters the Sound. The AOI then continues eastward along the southern shore of Albemarle Sound, extending south of the sound anywhere from 2-10 kilometers, and including Bull Bay and the Scuppernong River. The AOI turns south covering the western shore of the Alligator River inlet of Albemarle Sound (and extending 8 kilometers back to the west). At the south end of the Alligator River inlet, the AOI narrows considerably, wraps around the south end of the inlet and heads back north to circle clockwise around the small peninsula at the southeast edge of Albemarle Sound. The center of this peninsula, excluded from the AOI, is marked on maps as the Dare County Bombing Range. The AOI heads back south along Croatan Sound, again capturing Sound-facing lands extending inland roughly 5-10 kilometers. As the AOI curves towards the southwest, it forms the northern shore of Pamlico Sound, and includes the Long Shoal River inlet, Wysocking Bay, Jupiter Bay, and most of the Swanquarter NWR. The AOI bends around the south side of Lake Mattamuskeet, but excludes it (as part of the large northern peninsula's interior) to focus on the near-shore lands between the lake and Pamlico Sound. As the AOI moves further west, it winds around both Rose Bay and the Pungo River's inlet, capturing a complex network of tributaries of the Pungo and Pamlico Rivers. The AOI captures the upper estuary waters of the Pungo River, and it is here that a narrow AOI corridor cuts back to the northeast to connect with the AOI at the southern end of the Alligator River inlet. This creates a "doughnut hole" within the AOI around Lake Mattamuskeet and the Bombing Range referenced above. The AOI continues west to capture the area where the Tar River widens (at Washington, NC) and becomes the Pamlico River. On the South side of the Tar / Pamlico River, the AOI then heads southeast encompassing the shorelines and shore lands of Chocowinity Bay, Blounts Bay, Durham Creek, South Creek, and the extensive Goose Creek drainage. The AOI then encompasses Goose Creek Island, including Mouse Harbor and Jones Bay. The AOI extends a narrow "finger" 12 kilometers out into Pamlico Sound to the southeast of Goose Creek Island. The AOI then extends to the southwest, capturing the shoreline lands and islands around Bay River, as well as the small peninsula that separates Bay River from the larger Neuse River to the south. The AOI then extends to the west to capture both the north and south shorelines of the Neuse River inlet to Pamlico Sound. At its westernmost extent, the AOI encompasses the town of New Bern, NC and the area where the Trent and Neuse Rivers enter the Pamlico Sound system. Along the south shore of the Neuse River, the AOI includes

most of the Marine Corps Air Station Cherry Point, and the creek drainages to its east and west, Clubfoot Creek, Adams Creek (and the Intracoastal Waterway connecting to NC1901), South River, and Piney Island (along with Turnagain Bay, portions of West Bay, and Long Bay. The AOI butts up against NC1901 to the south and east of Long Bay and West Bay.

On the Sound side throughout this Area of Interest, the AOI boundary extends out from the shore anywhere from just a couple hundred meters to more than a kilometer. The AOI, however, clearly excludes most of the deep water in these Sounds and deeper river inlets.

The AOI includes Albemarle and Pamlico Sound shoreline portions of Currituck, Camden, Pasquotank, Perquimans, Chowan, Bertie, Washington, Tyrrell, Dare, Hyde, Pamlico, Craven, and Carteret Counties in North Carolina.

The project is located approximately between 34°51'39"and 36°24'55" North Latitude, and 75°42'25" and 77°08'52" West Longitude.

For the context of this specific Project Area report, it is important to understand that the NC1903 Project Area has two sibling Project Areas (NC1901 & NC1902) immediately contiguous and to its northeastern-most edge (near Currituck Sound), and along its southeastern-most edge (north of Beaufort, NC).

Imagery

The photography used in the aerotriangulation phase was flown by Quantum Spatial and consisted of one hundred and one (101) flight lines. The photographs were acquired at a nominal ground sample distance of 0.33 meters using the Leica ADS100 push broom sensor. The 4band color photographs were acquired by Quantum Spatial between January 5, 2020 and April 17th, 2020. All imagery was acquired using >30% side overlap, sun angles >20 or >25 degrees (depending on the date of acquisition). The layout of the photographs is shown in the attached diagrams. Photographic coverage, resolution, overlap, and metric quality were adequate for the performance of the aerotriangulation phase. Additional information can be found in the NC1901 \ NC1902 \ NC1903 Acquisition Summary report.

Control

A combination of photo identifiable ground control points and Airborne GPS/IMU data were used to control the imagery for aerotriangulation.

A. Airborne GPS/IMU: Airborne GPS and IMU data were collected and processed by Quantum Spatial and were used as control in the aerotriangulation, and inertial measuring unit (IMU) measurements were used to refine these.

B. Ground Points: QSI was dispatched to survey one hundred thirteen (113) photo ID control points (horizontal and vertical), and 5 check points. Five surveyed points were used to check the horizontal and vertical accuracy of the aerotriangulation. The results of the survey have been published in the final ground control report that has been included in this Aerotriangulation submission to NGS.

   Overall, the ground control points were found to be adequate to supplement the airborne GPS control.

Methodology

The photographs were bridged using digital aerotriangulation methods to establish the network of photogrammetric control required for the compilation phase. The images were bridged in a bundle adjustment that included all 101 4Band color non-tide coordinated images. Measurements were made utilizing a digital photogrammetric workstation running the Windows 10 operating system. Leica's XPRO Aerotriangulation software was used to perform automatic point measurements and interactive point measurements of tie points. The final adjustment of the block was accomplished by using a rigorous simultaneous least squares bundle adjustment, and analysis tools within XPRO were used to refine the aerotriangulation solution and to evaluate the accuracy of the adjustment.

Analysis of Results

The final XPRO results were evaluated for the triangulation adjustment providing a display of the image and point residuals and connections between frames. Weak points and blunders were identified and corrected. The final aerotriangulation solution for the image block was computed in XPRO as a full bundle block adjustment. The RMS of the standard deviations in both X and Y directions were calculated and used to determine the radius of the 95% confidence circle for each image block. The predicted horizontal circular error accuracy (RMSE or 95% CI) is 0.34m for the 4band photos. (see Annex 3 for details of the computations). This accuracy refers to the overall block, but in the bundle adjustments the error was distributed such that the largest errors are associated with points around the edges of the project and areas of vast water where the strength of the solution is weakest, while points down the middle of each block located on areas of extensive land cover have the smallest errors because those points are measured on a greater number of images. In addition, each of the five (5) ground control check points measured in and the coordinates and elevations of these check points were not constrained at all in any of the block adjustments, but were treated as pass points, and adjusted coordinates were computed and the differences are shown below:

		4Band	
POINT ID	**ΔX M**	**ΔY M**	**ΔZ M**
T142B	-0.023	-0.129	0.252
AT329A	-0.032	-0.240	-0.073
AT313A	0.194	-0.119	0.225
AT201	-0.075	0.127	0.099
AT109B	0.266	-0.161	0.048

As a final check select strips of photography were examined in XPRO QCViewer to ensure the horizontal and vertical integrity of the XPRO solution, and to verify the suitability of the database for use in the compilation phase. The images were checked for proper parallax, ground control tolerance, and check point tolerance. Models covering the four check points referenced above were specifically reviewed in this manner, and included the following:

Point ID	Flight Lines & Images	Image Dates
T142B	930082	01-06-2020
AT329A	930057	03-02-2020
AT313A	930007	04-17-2020
AT201	930005	02-08-2020
AT109B	930082	01-06-2020

To conclude, the aerotriangulation block meets the horizontal standards set forth b930007y NOAA in Chapter I of the Version 14A Statement of Work for Shoreline Mapping.

Project Database

A project database containing the following files has been included in this submittal.

- Exposure Stations
- Electronic Exposure Data (EED)
- Camera calibration data
- Ground Control File
- Ground Control Report
- Airborne GPS Control File and IMU Orientation Original DG
- RGB/NIR Stereo Imagery
- RGB/NIR Stereo Imagery Metadata
- Flight Line and Frame Shapefile
- Airborne Positioning and Orientation Report (APOR)
- Acquisition Summary Report
- AT Report

Positional data is based on the North American Datum of 1983 (NAD83 (2011)), and is referenced to the Universal Transverse Mercator (UTM) Zone 18 coordinate system

ANNEX 1 – Control Diagram

Project Control Diagram

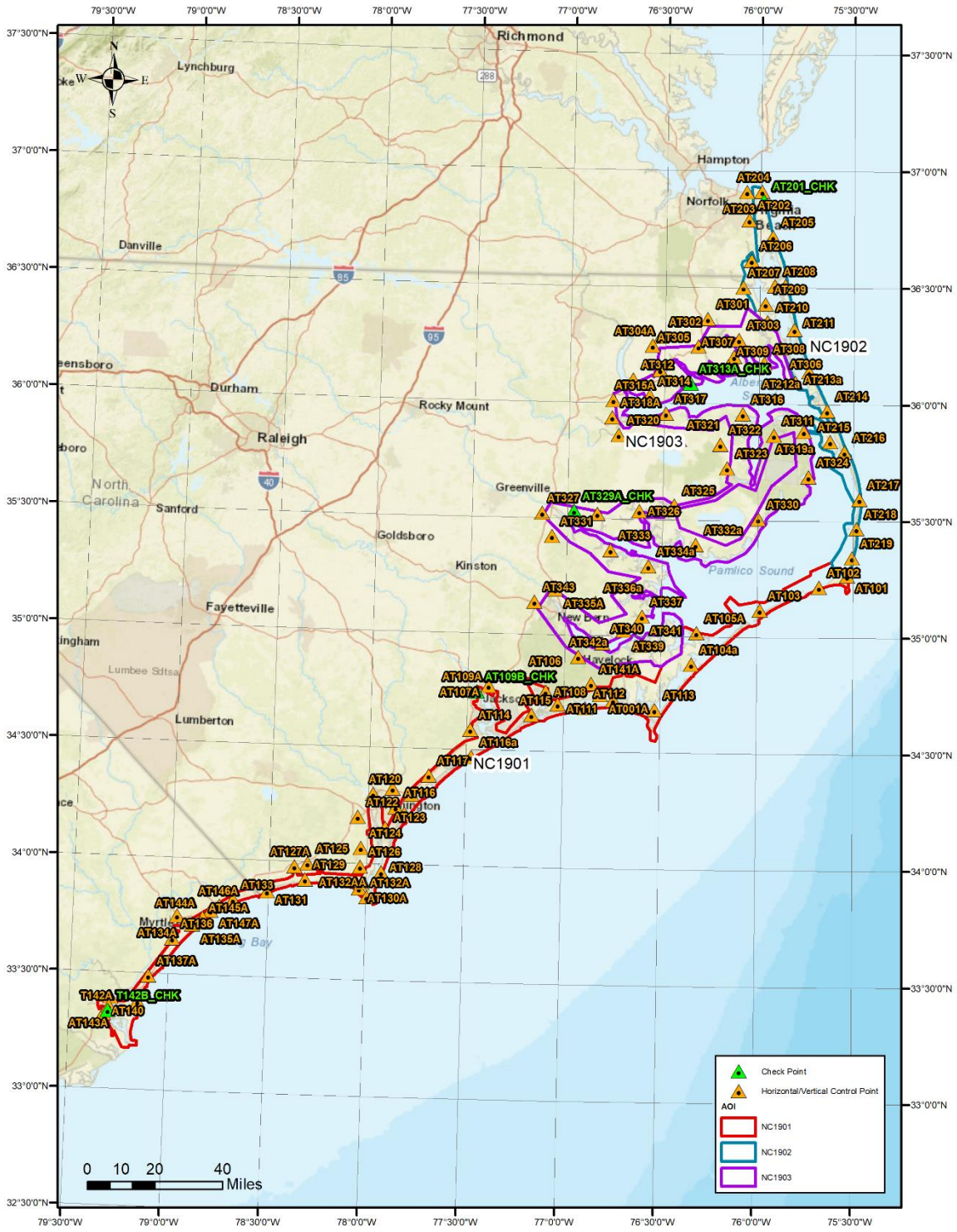

ANNEX 2 – 4Band – Flight Lines

Flight Line Diagram – 4 Band

NC1901 / NC1902 / NC1903

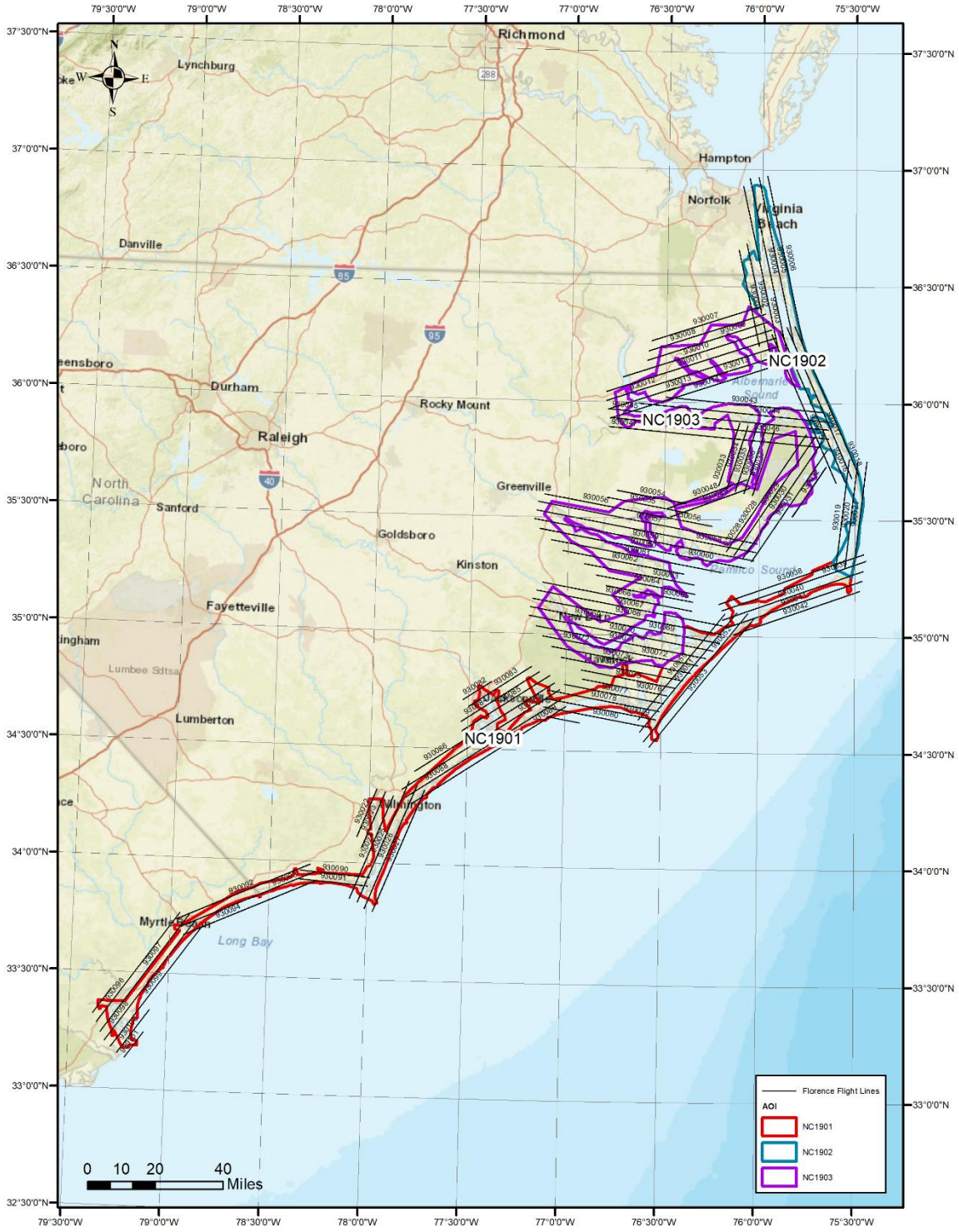

ANNEX 3 - Horizontal Accuracy Computation

The Horizontal Accuracy Statement reported in the Analysis of Results is based on the predicted circular horizontal accuracy of adjusted points in the aerotriangulation solution. This circular accuracy equals the radius of the 95% confidence circle as calculated from the horizontal (x and y) root-mean-square (RMS) values of the standard deviations for all triangulated ground points, rounded to the nearest tenth of a meter.

The root mean square of all standard deviations of triangulated ground points:

Block 1 (NC) RMS(x) =0.1530 meters RMS(y) =0.1840 meters

The value for the confidence circle radius is given by the following expression:

R=K*Sx

Where Sx is defined as the larger of the two (X and Y) RMS values, and K is interpolated using the C ratio from the Table of Cumulative Probability.

The C ratio equals the smaller of the RMS values divided by the larger:

Block 1 (NC): C=0.1530/0.1840 = 0.831522

The following line (95% probability level) from the Table of Cumulative Probability was used to determine the value of K by a simple linear interpolation between the two nearest values of C:

C	0	.1	.2	.3	.4	.5	.6	.7	.8	.9	1.0
K(95%)	1.95996	1.96253	1.97041	1.98420	2.00514	2.03586	2.08130	2.14598	2.23029	2.33180	2.44775

Block 1 (NC)

K =2.23029+ [(.831522 -0.8) / (0.1) * (2.33180 - 2.23029)]

=2.23029+ (.032 * 0.10151)

=2.23029+ .0324832

K =2.23029=2.262538

R = K * Sx = 2.262538 * 0.1840 = .42

The Radius of the 95% Confidence Circle 0.42 **meters**.